

Published in final edited form as:

Adv Phys Org Chem. 2011 January 1; 45: 39–91. doi:10.1016/B978-0-12-386047-7.00002-3.

The Generation and Reactions of Quinone Methides

Maria M. Toteva and John P. Richard

Department of Chemistry, University at Buffalo, Buffalo, NY, 14260, USA

1. Introduction

The 1,2- and 1,4 quinone methides are formally neutral molecules. However, the zwitterionic aromatic valence bond resonance structures (Scheme 1) make an important contribution to their structure. This combination of neutral and zwitterionic valence bond structures confers a distinctive chemical reactivity to quinone methides, which has attracted the interest of many chemist and biochemists.

The neutral 1,4 and 1,2 quinone methides react as Michael acceptors. However, the reactivity of these quinone methides is substantially different from that of simple Michael acceptors. The 1,6-addition of protonated nucleophiles NuH to simple Michael acceptors results in a small *decrease* in the stabilization of product by the two conjugated π -orbitals, compared to the more extended three conjugated π -orbitals of reactant. However, the favorable ketonization of the initial enol product (Scheme 1) confers a substantial thermodynamic driving force to nucleophile addition. By comparison the 1,6-addition of NuH to a 1,4 quinone methide results in a large *increase* in the π -stabilization energy due to the formation of a fully aromatic ring (Scheme 2A). This aromatic stabilization is present to a smaller extent at the reactant quinone methide, where it is represented as the contributing zwitterionic valence-bond structure for the 4-O⁻-substituted benzyl carbocation (Scheme 1). The ketonization of the product phenol (Scheme 2B) is unfavorable by ca 19 kcal/mol.^{1,2}

Quinone methides are highly reactive and this reflects the large contribution of the polar zwitterion to the overall molecular structure (Scheme 1). In other words, the 1,4 quinone methide is a benzylic carbocation that is strongly stabilized by the resonance electron donating 4-O⁻ substituent.³ Consequently, the rate constants k_{Nu} for addition of nucleophiles to a di-CF₃ substituted quinone methide (Scheme 3A) are correlated by the N⁺ scale for nucleophile addition to strongly resonance stabilized carbocations,^{4,5} and quinone methides have been used by Mayr, alongside other carbocations, as reference electrophiles in the construction of nucleophilicity scales.⁶ The efficient and synthetically useful 2 + 4 addition of electron-rich alkenes to 1,2 quinone methides can be similarly understood as the stepwise electrophilic addition of a resonance stabilized benzylic carbocation to nucleophilic alkene, followed by capture of the oxocarbenium ion intermediate by phenoxide ion (Scheme 3B).⁷

1,3-Quinone methides are strikingly different from the 1,2- and 1,4-isomers, because there is no direct orbital interaction between the *meta*-oxygen and carbon substituents at the benzene ring. Consequently, the neutral valence bond resonance form for the 1,3-quinone methide is a triplet biradical (Scheme 1). These 1,3-quinone methides are chemically more unstable and difficult to generate than their 1,2- and 1,4-isomers, which exist as stable neutral molecules.⁸

This chapter will focus on *o*- and *p*-quinone methides and will be divided into two parts. The first will present methods for generating quinone methides in photochemical and solvolysis reactions and will emphasize how the structure and stability of quinone methides dictates the pathways for their formation. The second section will discuss the results of experiments to characterize the reactivity of quinone methides with nucleophilic reagents, and the broader implications of these results. The scope of this presentation will reflect our interests, and

will focus on studies carried out at Buffalo. We considered briefly writing a comprehensive chapter on quinone methides, but abandoned this idea when we learned of Steve Rokita's plans to edit a 12-chapter text, which presents an extremely comprehensive coverage of the chemistry and biochemistry of quinone methides.⁹

2. Generation of Quinone Methides by Photochemical Reactions

Absorption of a photon in the UV spectral region may lead to generation of electrophilic species by fast heterolytic bond cleavage at the photochemically excited state.¹⁰ Quinone methides are readily accessible through reactions of such photochemical excited states.^{11,12} This section outlines photochemical pathways for the generation of quinone methides.

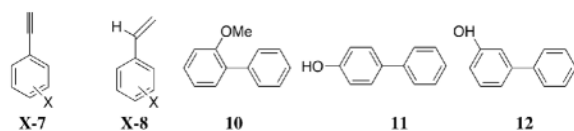
Early Work

Lactones undergo a variety of competing photochemical reactions to give complex mixtures of products.¹³ However, irradiation of pent-3-en-4-olide at 77 K in an IR cell gives the methyl vinyl ketone and carbon monoxide as the initial photochemical reaction products (Scheme 4A).¹⁴ Benzofuran-2(3H)-one (Scheme 4B, X = O) undergoes a related photochemical decarbonylation to give an *o*-quinone methide **1**, which can be trapped by 1,1-dimethoxyethene methanol to form the *o*-hydroxybenzylmethyl ether or by a ketene acetal to form an *ortho*-lactone (Scheme 5A).¹⁴ The photochemical reaction of 3-phenylisocoumaranone in methanol gives the *o*-quinone methide *o*-**2** (Scheme 4C) which then reacts to form xanthene (**3**, Scheme 5B). Xanthene was proposed to form by intramolecular electrocyclic addition reaction of *o*-**2** followed by a 1,3 hydrogen shift (Scheme 5B).¹⁵ The photochemical decarbonylation of 2,4,5-trimethylhomogenistic lactone gives the 2-hydroxy-1,3,4-trimethyl-*o*-quinone methide.¹⁶ The *o*-thioquinone methide has been generated by decarbonylation of benzothiolactone (Scheme 4B, X = S) and trapped by *N*-ethylmaleimide.¹⁷

Irradiation of 2,2-dimethylchromene through pyrex using a 550W Hanaovia lamps initiates a retro 4 + 2 reaction to form the extended quinone methide **4** which reacts with methanol to form a pair of methyl ethers (Scheme 6A).¹⁸ Flash photolysis of coniferyl alcohol **5** generates the quinone methide **6** (Scheme 6B) by elimination of hydroxide ion from the excited state reaction intermediate.¹⁹ The kinetics for the thermal reactions of **6** in water were characterized,²⁰ but not the reaction products. These were assumed to be the starting alcohol **5** from 1,8 addition of water to **6** and the benzylic alcohol from 1,6 addition of water (Scheme 6). A second quinone methide has been proposed to form as a central intermediate in the biosynthesis of several neolignans,^{21a} and chemical synthesis of neolignans has been achieved through a quinone methide that was proposed to form as an intermediate in their biosynthesis.^{21b}

Photoprotonation of alkenes

Phenylacetylenes **X-7** and styrenes **X-8** undergo photoprotonation in aqueous sulfuric acid followed by addition of water to give the corresponding ring substituted 1-phenylethanols and ring-substituted acetophenones, respectively.²² Photoprotonation by laser flash photolysis has been used extensively a source of benzylic and other carbocations in studies to characterize their thermal reactivity with solvent and added nucleophilic reagents.^{10,23,24}



Yates and coworkers have examined the mechanism for photohydration of **o-OH-8**. The addition of strong acid causes an increase in the rate of quenching of the photochemically excited state of **o-OH-8**, and in the rate of hydration of **o-OH-8** to form 1-(*o*-hydroxyphenyl) alcohol. This provides evidence that quenching by acid is due to protonation of the singlet excited state **oOH-8*** to form the quinone methide **9**, which then undergoes rapid addition of water.²² Figure 1 shows that the quantum yields for the photochemical hydration of *o*-methoxystyrene (closed circles) and *o*-hydroxystyrene (open circles) are similar for reactions in acidic solution; but, the quantum yield for hydration *o*-hydroxystyrene levels off to a pH independent value at around pH 3, where the yield for hydration *o*-methoxystyrene continue to decrease.²⁵ The quantum yield for the photochemical reaction of *o*-hydroxystyrene remains pH-independent until pH \approx p*K*_a of 10 for the phenol oxygen, and the photochemical efficiency of the reaction then decreases, as the concentration of the phenol decreases at pH > p*K*_a = 10.²⁵ These data provide strong evidence that the *o*-hydroxyl substituent of substrate participates directly in the protonation of the alkene double bond of **o-OH-8*** (*k*_{iso}, Scheme 7), in a process that has been named “excited state intramolecular proton transfer” (ESIPT).²⁶

A quinone methide makes a surprising appearance as an intermediate of the photochemical exchange of deuterium from D₂O into the 2'-position of 2-phenylphenol (**13**).²⁷⁻²⁹ No photochemical deuterium exchange is observed for reactions of the related phenylanisole **10** or phenylphenols **11**, and **12**; and, deuterium exchange at the 4'-phenyl position of **13** is very much slower than deuterium exchange into the 2'-phenyl position. These observations provide evidence that the 2-OH plays a direct role in the deuterium exchange reaction. They are consistent with Scheme 8, where deuterium exchange at the 2'-position of **13** proceeds with intramolecular protonation of the phenyl ring by the neighboring -OD group.²⁸ The efficiency of deuterium exchange into both the 2'- and 4'-phenyl positions in mixed water/acetonitrile solvents increases with increasing D₂O composition of the solvent. The maximum efficiency for exchange into the 2'-phenyl position is observed at very low \approx 0.1 M concentration of D₂O, while a much higher concentration of 10 M D₂O is required to obtain the maximum efficiency for exchange into the 4'-phenyl position.²⁸ This is consistent with deuterium exchange into the 2'-phenyl position by direct photochemical excitation of the phenol ring in a reaction that does not depend strongly on the solvent polarity (Scheme 8), and with exchange into the 4'-position that proceeds with excitation of the phenoxide ion that is stabilized in solvents of high D₂O composition.

Photoheterolysis Reactions

There have been many reports of photosolvolysis of benzyl alcohols and other benzyl derivatives to form the corresponding benzylic carbocation;³⁰⁻³³ and, photosolvolysis using laser flash photolysis has been used extensively a source of benzylic carbocations in studies to characterize their thermal reactivity with solvent and added nucleophilic reagents.¹⁰ Photolysis of substituted phenols that contain electron-withdrawing groups at the benzylic carbon has also been reported to give quinone methides.³⁴⁻³⁶ For example, Seiler and Wirz showed that irradiation of trifluoromethylphenol and trifluoromethylnaphthol in aqueous solution yielded the corresponding hydroxybenzoic acids and hydroxynaphthoic acids. It was proposed that photohydrolysis proceeds by breakdown of an excited state singlet with cleavage of the C-F bond to form the quinone methide shown in Scheme 9, which reacts rapidly with solvent to form *p*-hydroxybenzoic acid.³⁶

The photosolvolysis of *o*-hydroxybenzyl alcohols in 50/50 methanol/water is faster than photosolvolysis of the corresponding *o*-methoxybenzyl alcohol, because ionization of the phenol oxygen strongly activates these substrates for loss of hydroxide ion to form quinone methides.³⁰ The quantum yield for conversion **14** to **15** ($\lambda_{\text{max}} = 450$ nm) by laser flash

photolysis increases with increasing pH to a constant value at $\text{pH} \approx 3$; a further increase is then observed at $\text{pH} > 8$.¹¹ The first rise in quantum yield was proposed to represent the increase in the photosolvolytic reactivity of the first excited state that accompanies deprotonation of phenol oxygen ($\text{p}K_{\text{a}} \approx 2$, bottom pathway, Scheme 10), and the second rise to represent an additional pathway for formation of the quinone methide by direct excitation of the ground state of phenoxide ion (bottom pathway, Scheme 10), whose $\text{p}K_{\text{a}}$ of 10 is much higher than for the singlet excited state.³⁷

There are many additional reports of the of *o*- and *p*-quinone methides in photosolvolytic reactions.

- a. Photolysis of (1-phenyl)(1-*o*-hydroxyphenyl)ethene and 1-(*o*-hydroxyphenyl)(1-phenylethanol) in 1/1 acetonitrile/water results in photoprotonation and photosolvolytic reactions, respectively, to form the relatively long-lived ($t_{1/2} > 100$ μsec) quinone methide **15a** (Scheme 11A).³⁸
- b. Laser flash photolysis of biphenyls **16** and **17** produces the corresponding quinone methides **15b** and **15c**, respectively (Scheme 11B and 11C).²⁹
- c. Laser flash photolysis of the acetate ester of (*p*-hydroxyphenyl)(*p*-methoxyphenyl)-methanol gives the quinone methide **20** (Scheme 11D).³⁹
- d. Photosolvolytic of vitamin B₆ in methanol produces the corresponding methyl ethers, consistent with the formation and thermal trapping of the pyridine *o*-quinone methide **18**.^{40,41} The trapping of **18** by ethyl vinyl ether was also reported (Scheme 11E).^{40,41}

Freccero and coworkers have reported the photochemical generation of quinone methide **20** from the racemic binaphthol **19a**, and they have adopted this reaction to generate chiral ligands with potential applications in organic syntheses.^{42,43} The trapping of **20** by L-proline methyl ester, followed by a second round of quinone methide generation and trapping with L-proline methyl ester gives a diastereomeric mixture of binaphthols **21 (R,R, S)** and **21 (R,R, R)** labeled with proline methyl ester at the 3 and 3' positions (**21**). Resolution of these diastereomers, followed by photochemically driven stepwise substitution of proline methyl ester by nucleophilic amines, thiols or water afforded a series of optically pure binaphthols **19b** (Nu = -NEt₂, morpholine, -NPh₂ -S(CH₂)₂OH, -OH) in > 99% enantiomeric excess (Scheme 12).⁴³ The binol quinone methides generated from **19a** have been used as reagents to cross-link DNA.^{42a} The role of quinone methides in the sequence specific alkylation of DNA has also been investigated.^{42b}

The solvolysis reactions of 9-substituted fluorenes have been examined in studies to characterize the effect of the delocalized 12- π cyclic array of electrons on the stability of the 9-fluorenyl carbocation reaction intermediate.⁴⁴⁻⁴⁷ 1,1-Diphenylmethanol does not undergo photosolvolytic in 50% methanol/water under conditions that lead to extensive photosolvolytic of fluorenyl. This provides evidence for an enhanced rate of formation of the photochemical excited state of carbocations which contain a conjugated cyclic 4n π -array of electrons.⁴⁸ The *o*-quinone methide intermediate of photosolvolytic of 1-hydroxyfluorenyl, **22**, has a relatively long lifetime of 5–10 s in neat H₂O (Scheme 13A).⁴⁹ No *m*-quinone methide intermediate **23** could be detected from photosolvolytic of 2-hydroxyfluorenyl using laser flash photolysis, but the intermediate of photosolvolytic of α -phenyl 2-hydroxyfluorenyl decays with a lifetime of 66 ns in 1:4 acetonitrile/water that is similar to the lifetime for the parent α -phenyl fluorenyl carbocation.⁴⁹ These data show that there is strong stabilization of the cationic fluorene carbon by electron-donation from the *o*-oxygen (Scheme 13A). There is much weaker electron donation from the *m*-oxygen because the neutral valence bond resonance structure for quinone methide **23** contains fewer

aromatic 6π rings [zero] than the carbocation zwitterion [two, Scheme 13B). Consequently, the structure and reactivity of the intermediate of the photosolvolysis reaction shown in Scheme 13B has a reactivity similar to that for a simple *m*-substituted fluorenyl carbocation.⁴⁹

Kresge and coworkers, and McClelland³⁹ have generated *o*-quinone methide,^{50,51} *p*-quinone methide⁵² and related simple quinone methides as products of photolytic cleavage of 2-hydroxybenzyl and 4-hydroxybenzyl derivatives.^{53–58} The results of studies on the mechanism for nucleophile addition to these simple quinone methides are summarized in latter sections of this chapter.

Other Photochemical Reactions

Photolysis of 5-methyl-1,4-naphthoquinone (**24**) gives 4-hydroxy-5-methylidene naphthalen-1(*5H*)-one (**25**) in the ground state within 2 ps of excitation, with a quantum yield of 1.0.⁵⁹ Formally, this is a photoenolization reaction; however, the product of the reaction also has quinone methide functionality, and zwitterionic resonance structures can be written for **25** that place positive charge at either the methide or benzylic carbon (Scheme 14). There is strong specific acid catalysis of the addition of nucleophiles due to protonation of the quinone oxygen (Scheme 14). The pH rate profile for nucleophile addition shows a downward break at low pH, and the fit of the experimental data gives a $pK_a = 1.1$ for protonation of the quinone oxygen [Scheme 14].⁵⁹

4-Hydroxyphenacyl acetate undergoes photochemical solvolytic rearrangement in aqueous acetonitrile to form 4-hydroxyphenylacetic acid.⁶⁰ The first step in this reaction is formation of a singlet excited state intermediate, and the final steps almost certainly involve addition of solvent to a spiro-quinone intermediate **26**. This spiro-quinone might form directly in a reaction where heterolytic photolytic bond cleavage is concerted with addition of the β -carbon to the hydroxyphenyl ring (Scheme 15, upper pathway). However, the investigators favored a more complex mechanism in which the excited state undergoes intramolecular proton transfer through a water chain to form quinone methide **27**, which subsequently undergoes rearrangement to a spiro intermediate (Scheme 15, lower pathway).⁶⁰

Xanthene (**28**) undergoes photoisomerization in acetonitrile/water to give mainly 6*H*-dibenzo[*b,d*]pyran **31** along with low yields of **29** and **32**. It was proposed that photexcitation is followed by homolytic bond cleavage to form a diradical, which partitions between hydrogen abstraction to give **29** and rearrangement to a mixture of *cis* and *trans* quinone methides **30** (Scheme 16A).^{61a} These quinone methides partition between addition of solvent water to form **32** [**33** in methanol solvent] and ring closure to form **30**. It was shown in a separate experiment that **30** and **33** undergo a rapid photochemically driven interconversion in methanol to reach a steady state concentration of $[\mathbf{33}]/[\mathbf{31}] = 55/45$ (Scheme 16B).^{61a}

Photolysis of *o*-hydroxyphenyl benzyl alcohol **34** gives mainly **31** in a reaction that proceeds with high overall conversion of reactant to products (71%), but with low ($\Phi = 0.0073$) quantum yield.^{61a} No xanthene, which might form by loss of hydroxide ion from the photochemically excited state followed by cyclization of the *o*-phenoxy substituted carbocation, is observed. Similar products are observed from the reactions of **28** (Scheme 16) and **34** (Scheme 17) consistent with partitioning of the common quinone methide intermediate **30**. It was proposed that the excited state of **34** undergoes homolytic C–O cleavage to a radical pair, which recombine to form **35** and **36**. The *ortho*-adduct **35** then undergoes photoheterolysis to **30**, which is captured by water to give **32**; and, the *para*-adduct **36** tautomerizes to **37** (Scheme 17).^{61b}

Irradiation of 3-hydroxy-2-naphthalenemethanol and 2-hydroxy-1-naphthalenemethanol results in efficient dehydration and the formation of isomeric naphthoquinone methides, 2,3-naphthoquinone-3-methide and 1,2-naphthoquinone-1-methide respectively (Scheme 18).⁶² These quinone methides were trapped by azide anion, thiols and vinyl ethers.

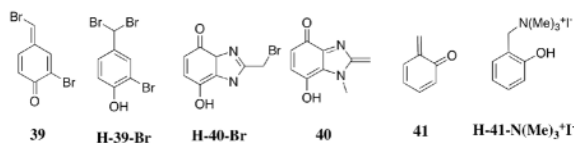
3. Generation of Quinone Methides by Heterolytic Bond Cleavage

Direct Methods

Many halide and ester derivatives of *p*-OH- and *o*-OH-substituted benzyl alcohols undergo stepwise S_N1 (D_N + A_N)⁶³ nucleophilic substitution reactions through quinone methide intermediates (Scheme 19). These species accumulate in weakly nucleophilic reaction medium, but are very difficult to isolate. The preferred pathway for quinone methide formation depends upon the reaction pH. In strongly acidic solutions, heterolytic C-X bond cleavage at **H-38-X** to form **H-38⁺** is followed by thermodynamically favorable loss of a to form the *p*-hydroxybenzyl cation **H-38⁺**. This activation is estimated as *ca* 10⁸-fold from the Hammett reaction constant *p* = -6 for solvolysis of 1-phenylethyl,⁶⁴ and cumyl⁶⁵ derivatives, and the difference in the Hammett substituent constants for the *p*-OH ($\sigma^+ = -0.90$) and the *p*-O⁻ substituents ($\sigma^+ = -2.2$).⁶⁶ The activation is so great that solvolysis may proceed by the reaction of **⁻38-X**, even in acidic solutions where the concentration of **⁻38-X** is very low.⁶⁷

There are many reports of generation of quinone methides by heterolytic bond cleavage at *p*-OH and *o*-OH substituted benzyl derivatives.

1. 2,6-Dimethyl quinone methide (**38a**, R₁ = CH₃, R₂ = H) was one of the first spectroscopically characterized “simple” quinone methides. This quinone methide was generated in alkaline aqueous solution from chloride and acetate precursors **H-38a-Cl** and **H-38a-OAc**.⁶⁸ Stable quinone methides such as **38b-e** (Scheme 19) were generated from chloride precursors **H-38-Cl**.^{69,70}
2. The quinone methide **39** was generated as an intermediate of the solvolysis of **H-39-Br** in aqueous dioxane.⁷¹ The conversion of **H-40-Br** to quinone methide **40** in acidic, neutral and alkaline aqueous solutions, and the trapping of **40** by nucleophiles has been examined.^{72,73}
3. The tetramethyl quinone methide **38f** has been generated by cleavage of the chloride precursor in dichloromethane, and its reactions with amine bases studied.⁷⁴
4. The *o*-quinone methide **41** was generated by cleavage of (2-hydroxybenzyl)-trimethylammonium iodide (**H-41-N(Me)₃⁺ I⁻**) in hot aqueous solution. The products of trapping of **41** by oxygen, sulfur and nitrogen nucleophile were characterized.⁷⁵



4. Generation of Quinone Methides by Unmasking a Quinone Oxygen

There are several reports of the generation of quinone methides from precursor benzyl derivatives, where an O-protecting group is first removed from the quinone oxygen and the resulting 2- or 4-hydroxy benzyl derivative undergoes rapid cleavage to form the quinone methide (Scheme 20). There is a requirement that the rate of both the deprotection and

solvolysis step be rapid, if the kinetically unstable quinone methide is to accumulate. Although there is not an absolute requirement for their use,^{76a} the high catalytic activity of enzymes makes them effective reagents in the deprotection of precursors to quinone methides. For example, acid phosphatase removes the protecting phosphate from *p*-fluoromethylphenyl phosphate **42** to give 4-hydroxybenzyl fluoride, which then reacts with loss of HF to form quinone methide **43** (Scheme 20A).^{76–78} Ribonuclease was used to remove a uridyl protecting group from **44** to form 4-hydroxybenzyl fluoride, which likewise breaks down to **43** (Scheme 20B).⁷⁹

The enzymes used to generate reactive quinone methides often undergo inactivation by addition of this electrophile to essential nucleophilic amino acid side chains of the protein catalyst. This is a type of suicide enzyme inhibition.⁸⁰ This was observed for the acid phosphatase and ribonuclease catalysts used to generate **43**.^{76–79} Alkaline phosphatase has been used to remove the phosphate protecting group from a derivative of an *o*-difluoromethylphenyl phosphate that was covalently attached to a solid support. Breakdown of the immobilized 4-hydroxybenzyl difluoride gives an immobilized quinone methide that, in principal, will react irreversibly with proteins and lead to their attachment to the solid supports.⁸¹

Taylor and coworkers have prepared *o*-fluoromethyl and *o*-difluoromethyl estrone sulfates⁸² and shown that these compounds are good substrates for steroid sulfatases.⁸³ The phenol product of hydrolysis of *o*-fluoromethyl estrone sulfate undergoes heterolytic cleavage to form a quinone methide which inactivates the steroid sulfatase (Scheme 20C).⁸³ The phenol product of hydrolysis of *o*-difluoromethyl estrone sulfate breaks down first to a quinone methide and then to the *o*-formyl estrone, which also inactivates the steroid sulfatase.⁸³

The silyl group is widely used as an oxygen-protecting group, because of the ease of its removal by nucleophilic substitution by fluoride anion. The protected phenols *O*-(*tert*-butyldimethylsilyl)-*p*-(bromomethyl)phenol (**45**) and *O*-(*tert*-butyl-dimethylsilyl)-2,6-bis(bromomethyl)phenol (**46**) react rapidly with fluoride anion in water to form the corresponding phenols, which then breakdown to the *ortho*-quinone methide **41** (Scheme 21A) and the substituted *ortho*-quinone methide **47**, respectively (Scheme 21B). These quinone methides rapidly alkylate nucleic acids.^{84,85} Crosslinked products are obtained from the reaction of **47** with DNA, because the first nucleophile addition of the first DNA nucleophile triggers cleavage of the product bromide to form a second quinone methide, which is trapped by a second tethered DNA nucleophile (Scheme 21C).⁸⁶

5. Generation of Quinone Methides by Nucleophilic Aromatic Substitution of Water at Carbocations

Solvolysis of **Me-48-OTs**, in ethanol gives two products; the ethyl ether (**Me-48-OEt**) from nucleophilic substitution of solvent at the benzylic carbon, and **Et-48-OEt** from nucleophilic substitution at both the benzylic carbon and C-4 of the aromatic ring (Scheme 22).⁸⁷ This result shows that the large destabilizing interaction between the electron-withdrawing α -CF₃ substituents and the cationic benzylic carbon at **Me-48⁺** is relieved by delocalization of charge onto the methoxyphenyl ring (Scheme 22).^{87–90} The effect of this delocalization of charge is to cause the C-4 ring carbon and the benzylic carbon of **Me-48⁺** to show similar electrophilic reactivity toward addition of the nucleophilic solvent ethanol.

Solvolysis of **Me-48-OTs** or **Me-48-Br** in 50/50 (v/v) water/trifluoroethanol proceeds through the carbocation intermediate **Me-48⁺** which, likewise, partitions between addition of water at the benzylic carbon to form **Me-48-OSolv** and at the C-4 ring carbon to form the hemiacetal **49**, which rapidly breaks down to the quinone methide **48**.⁸⁹ This quinone

methide has been characterized by ^1H NMR,⁸⁹ and its reactions with nucleophilic reagents were studied.^{4,67,91} The carbocation **Me-48⁺** was generated from **Me-48-Br** by laser flash photolysis in water and found to decay with a first-order rate constant of $(k_s + k_s') = 2 \times 10^7 \text{ s}^{-1}$ (Scheme 23). The quinone methide **48** forms by the much slower breakdown of the hemiacetal **49**,⁹² which undergoes acid-catalyzed cleavage to form **48** ($k_H = 3.4 \times 10^3 \text{ M}^{-1} \text{ s}^{-1}$) and ionization of the ring hydroxyl ($\text{p}K_a = 11$) to form an oxyanion that is also rapidly cleaved to **48** ($k_o = 4.3 \times 10^6 \text{ s}^{-1}$).

6. Generation of Quinone Methides by Oxidation of Phenols

Quinone methides form by two electron oxidation of *p*-hydroxy and *o*-hydroxy toluenes. This reaction proceeds by a complex mechanism through radical intermediates. There is evidence that single electron oxidation of 2,6-di-*tert*-butyl-4-methylphenol (**50a**) by ferricyanide or PbO_2 gives a benzyl radical, which isomerizes to the phenoxy radical **50b**.⁹³ The decay of **50b** was studied by ESR and other spectroscopic methods.⁹⁴ This reaction was second-order in **50b** and the rate constant was independent of the concentration of **50a** and the oxidizing agent PbO_2 .⁹⁴ This is consistent with disproportionation of **50b** to form the quinone methide **50c** (Scheme 24A). This mechanism was supported by the direct observation of quinone methide **50c** by UV spectroscopy. Quinone methides **50e** were generated by disproportionation of phenoxy radicals generated by the ferricyanide oxidation of 2,6-di-*tert*-butyl-4-isopropylphenol and 2,6-di-*tert*-butyl-4-*sec*-butylphenol (**50d**; R = H, CH_3 , Scheme 24B),^{95a} and detected by UV spectroscopy. The ether products **50f** of the trapping of **50d** by alcohols were characterized. Several quinone methides were prepared by silver oxide oxidation of precursor phenols in carbon tetrachloride,^{95b} where they are sufficiently stable to obtain NMR spectra.

Several general synthetic methods have been developed that utilize the novel reactivity of quinone methides generated by oxidation of phenol precursors. Angle and coworkers have generated 2,6-dialkyl or 2,6-dialkoxy substituted *p*-quinone methides **51** by oxidation of the corresponding phenols with Ag_2O . These undergo intramolecular addition to the carbonyl group or Michael acceptors in the presence of SmI_2 ,⁹⁶ where the quinone carbon reacts, formally, as a nucleophile in addition to the tethered electrophile. The SmI_2 acts as a reducing agent, and the mechanism of the cyclization reaction is thought to involve the reduction of the quinone methide to afford a radical anion/dianion, which then undergoes ring closure.⁹⁶ Angle and coworkers have also used quinone methides generated by oxidation of phenols in conventional cyclization reactions, where the quinone carbon reacts as an electrophile with tethered nucleophiles (*e. g.* Scheme 25B).⁹⁷

p-Quinone methides with chloro-, trichloro- and trifluoroethyl ester substituents (**52**) have been prepared by oxidation of the parent phenols. These react reversibly with weakly nucleophilic phosphodiester to form unstable adducts, which undergo intramolecular addition of the phenol oxygen to the neighboring activated acetyl group to give stable lactones (Scheme 25C).⁹⁸ Quinone methides **53** (Scheme 25D) were prepared in a similar fashion, and the products on addition of nucleophiles to the quinone carbon were isolated and characterized.^{99,100}

There is evidence that quinone methides form as intermediates in the metabolic oxidation of catechol derivatives, a key step in a variety of biosynthetic processes such as melanization and sclerotization of animal cells. Tyrosinase from mushrooms catalyses the oxidation of α -methyl dopa methyl ester **54a**. It has been proposed that this reaction observed *in vitro* is part of a metabolic pathway for the metabolism of **54a**. This reaction proceeds by oxidation of α -methyl dopa methyl ester **54a** to give **54b**, which cyclizes and is further oxidized to

quinone methide **54c** (Scheme 26).¹⁰¹ This quinone methide was identified by comparison to authentic **54c**, which was prepared by chemical oxidation of **54a** to **54c**.¹⁰²

7. Generation of Quinone Methides by Reductive Elimination Reactions of Quinones

We know of no examples of isomerization of methyl substituted quinones to the quinone methides (Scheme 27). On the other hand, quinone methides have been generated electrochemically by two electron reduction of α -methyl substituted 1,4-benzoquinones **55** (Scheme 28A, X = Cl, Br, OMe, OPh), followed by elimination of HX. For example, many naturally occurring quinone antitumor agents such as mitomycin C¹⁰³ and daunomycin¹⁰⁴ contain electron-withdrawing substituents that are positioned to undergo elimination after quinone reduction, to give reactive quinone methides that may be alkylated by DNA.¹⁰⁵

The mechanism for the generation of quinone methide **58** by reductive elimination of **55** has been investigated.¹⁰⁶ Single electron reduction by **55** by pulse radiolysis in water gives the semiquinone radical anion **56**, whose decay was monitored by transient absorption spectroscopy. This radical anion partitions between disproportionation to **60** and elimination to form the radical **58**. Disproportionation dominates at pH 7, but as the pH is lowered to 3 the competing elimination reaction to form the quinone methide radical **57** is observed for X = -OMe and -OPh. It was proposed that the product yields are controlled by the position of the equilibrium for protonation of **56** and that **56** undergoes mainly disproportionation, while **56** - the semiquinone radical **57** - undergoes mainly elimination of HX to give semiquinone radical anion **58** (Scheme 28). The quinone methide **59** is then formed by the one electron reduction of **58**.

Antitumor agents mitomycin A (**61A**) and mitomycin C (**61C**) contain a latent quinone functionality, which is exposed by reductive activation and elimination of a glycoside or an alcohol followed by opening of the aziridine ring. These quinone methides then react with nucleic acids to form *bis*-adducts.¹⁰³ The reductive activation of mitomycins provides selectivity in targeting solid tumors, because this is favored in the oxygen-deprived environment of tumor cells, and inhibited by the oxygen rich environment of healthy tissues.¹⁰⁷

The reductive activation of mitomycins in the cell is thought to be an enzymatic process.¹⁰⁸ Reduction of mitomycin A and C *in vitro* by H₂/PtO₂ or by Na₂S₂O₄ gives **62** which then breaks down to the quinone methide **63A**.¹⁰⁹ This quinone methide reacts with DNA to give a complex mixture of alkylated DNA and cross-linked oligonucleotides. Mitomycin A is both more easily reduced and more toxic than mitomycin C, and there is some evidence that the toxicity of mitomycin A is related to the greater ease of its *nonselective* reductive activation.¹⁰⁹ The Cr(ClO₄)₂-mediated reduction of mitomycin C in aqueous solutions to give **62C** has also been studied.¹¹⁰ McClelland and Lam examined the elimination of methanol from reduced quinone **62** and obtained strong evidence for a stepwise reaction mechanism through an iminium ion reaction intermediate (Scheme 29).¹¹¹

One interesting property of quinone methide **63** is that the terminal carbon of the extended conjugated system lies in *both* an extended quinone methide (carbons marked by +) and an extended enol (carbons marked by *). This carbon reacts as both a base, and undergoes protonation to form a quinone (upper pathway, Scheme 30A); and, as a Lewis acid in undergoing addition of nucleophilic reagents (lower pathway, Scheme 30A). Skibo and coworkers have examined the partitioning of the mitomycin analog **64** between *ketonization* to form a quinone and addition of chloride anion and thiol nucleophiles (Scheme 30B).⁷³

Reductive activation of quinones **65**¹¹² and **66**¹¹³ affords the novel cyclopropyl quinone methide alkylating agents **67** and **68** (Scheme 30C). These cyclopropyl quinone methides undergo protonation, nucleophile addition and complex ring expansion reactions [not shown]. The partitioning of **67** and **68** between these different reactions has been investigated.^{112,113}

Daunomycins are another class of anthracycline antitumor drugs that undergo reductive activation and elimination to form quinone methides that react with DNA. Chemical^{104,114,115} and enzymatic¹¹⁶ reduction of daunomycins **69** in water or a mixed water/DMF solvent gives hydroquinones **70**, which break down with elimination of the glycosyl leaving group to form quinone methides **71** (Scheme 31).

The terminal quinone methide of **71** is also the terminal carbon of an extended enol, and reacts as both a nucleophile and as electrophile (Scheme 32). This carbon shows a higher relative reactivity with electrophiles compared with nucleophiles than is observed for the corresponding terminal quinone carbon of mitomycins (Scheme 30A).⁷³ Furthermore, the addition of nucleophiles to **71** is readily reversible, but the nucleophile adduct can be trapped by reoxidation to form the quinone.¹¹⁷ The trapping of oxime and semicarbazone derivatives of **71** by intramolecular addition of the tethered nitrogen nucleophile to the quinone carbon has been reported,¹¹⁸ and the reaction of **71** with nucleophilic groups at DNA has been studied.^{119,120} Finally, the ambident nucleophilic/electrophilic reactivity of the quinone carbon of **71** is evident in the tendency of this quinone methide to form dimers (not shown).¹²¹

8. Other Pathways for Generation of Quinone Methides

Pyrolysis of *o*-hydroxybenzyl alcohol at 550 °C resulted in the formation of simple *o*-quinone methide which was directly observed using low-temperature IR spectroscopy.¹²² Pyrolysis of chroman (Scheme 33) at 400 – 600 °C gives the simple *o*-quinone methide and ethene along with *o*-cresol, benzofuran and styrene.^{123,124} The *o*-quinone methide was trapped with alkenes to form Diels-Adler adducts, with hydrogen gas or hydrogen atom to form *o*-cresol, or underwent a further pyrolysis to CO and fulvene.

In refluxing toluene or benzene, 4-allylcyclobutenones undergo ring expansion reaction to the corresponding *o*-quinone methides **72**, followed by a 1,5-hydrogen shift to give 2-ethenylphenols (Scheme 34A). This is a useful intermediate in the synthesis of highly substituted benzofuran derivatives.¹²⁵ Similarly **73** have been converted to quinone methides **74** where there is a trimethylsilyl group at the terminal alkylidene. These undergo methyl migration from silicon to carbon to form 1,2-benzoxasilols (Scheme 34B).¹¹⁷ The ((trimethylsilyl)methyl)-1,4-benzoquinones undergo desilylation in ethanol or aqueous acetonitrile to quinone methides **75** (Scheme 35), which were trapped by a vinyl ether (**76a**), acetate anion (**76b**) and ethanol (**76c**) (Scheme 36).¹²⁶

Quinone methides have been generated by reaction of their transition metal complexes.¹²⁷ The η^2 -coordinated complex **77** forms stable solutions in water and methanol. NMR spectroscopy showed that **77** and dibenzylideneacetone (DBA) in methanol undergo rapid conversion to **79** (Scheme 37). This is consistent with the reaction of DBA with the palladium ligand at **77** to give **78** and the palladium complex to DBA – the free quinone methide **78** is then trapped by methanol. A slower release of **78** from **77** is observed for the reaction in the presence of diphenylacetylene.¹²⁷

9. Structure-Reactivity Studies on Nucleophile Addition to Quinone

Methides

Our work on nucleophile addition to quinone methides is a direct extension of studies on the formation and reaction of ring-substituted benzyl carbocations,^{89,90,128–146} and have shown strong overlap with the interests of Kresge and coworkers. The main goal of this work has been to characterize the effect of the strongly electron-donating 4-O⁻ substituent on the reactivity of the simple benzyl carbocation, with an emphasis on understanding the effect of this substituent on the complex structure structure-reactivity relationships observed for nucleophile addition to benzylic carbocations.

10. O-Alkylation and O-Protonation of the Quinone Oxygen: Reactivity

Effects

The quinone oxygen of **p-1** is weakly basic. Protonation or methylation of this oxygen places a unit positive charge at **p-H-1⁺** or **p-Me-1⁺**, which is highly delocalized through the aromatic ring and onto the benzylic carbon. This increase in charge at the benzylic carbon leads to a large increase in the reactivity of this carbon with nucleophilic reagents that is consistent with a larger contribution of the aromatic valence bond resonance structure to the resonance hybrid structure of **p-H-1⁺** and **p-Me-1⁺** compared with **p-1** (Scheme 38). Kresge and coworkers have asked two questions in an effort to quantify the effect of O-protonation or O-alkylation on the structure and reactivity of **p-1**. (1) What is the basicity of the quinone oxygen of **p-1** compared with that of a quinone carbonyl group and phenoxide anion? (2) What is the effect of O-protonation and O-alkylation of **p-1** on the rate constant for addition of solvent to the benzylic carbon?

These questions were addressed in studies of the reactions of **p-1** and **p-Me-1⁺** in aqueous solution. The quinone methide **p-1** was generated by photolysis of neutral 4-hydroxybenzyl acetate in water, and $k_s = 3.3 \text{ s}^{-1}$ determined for addition of water.⁵² The O-methylated quinone methide **p-Me-1⁺** was generated as an intermediate of solvolysis of neutral precursors in water,¹²⁸ and $k_s = 2.5 \times 10^8 \text{ s}^{-1}$ for addition of water was determined by using the rate of diffusion-limited rate of nucleophile addition of azide anion to **p-Me-1⁺** as a clock for the slower addition reaction of solvent.^{135,138} These data show that methylation of **p-1** causes an enormous 6×10^7 -fold increase in the reactivity of the electrophile with solvent water.⁵²

The oxygen $\text{p}K_a$ of **p-H-1⁺** and the rate constant k_s for addition of solvent to this electrophile were determined by examining the effect of added hydronium ion on the observed rate constants for addition of water and of nucleophilic anions to **p-1** (Scheme 39). Figure 2 shows pL-rate profiles for water addition to **p-1** in H₂O and D₂O.⁵² The pH rate profile shows a good fit to eq 1 derived for Scheme 39 using $k_s = 3.3 \text{ s}^{-1}$ and $k_H = 5.3 \times 10^4 \text{ M}^{-1} \text{ s}^{-1}$.⁵² The absence a downward break at low pH in these pL profiles shows that $\text{p}K_a^{\text{H-1}}$ for **p-H-1⁺** is lower than the lowest pL examined in these experiments.

There are two reaction pathways for addition of neutral and anionic nucleophiles to **p-1** (Scheme 39): direct nucleophile addition with rate constant k_{Nu} ($\text{M}^{-1} \text{ s}^{-1}$) and specific acid-catalyzed nucleophile addition k_{HNu} ($\text{M}^{-2} \text{ s}^{-1}$), through the protonated intermediate **p-H-1⁺** with an acidity constant $K_a^{\text{H-1}}$ and microscopic rate constants of k_s' and k_{Nu}' (Scheme 39) for addition of solvent or nucleophilic anion to form product. Eq 2a and 2b show the relationships between the experimental rate constants k_H and k_{HNu} and the kinetic and thermodynamic parameters from Scheme 39.

$$k_{\text{obsd}} = k_s + k_H [H^+] \quad (1)$$

$$k_H = k_s' / K_a^{H-1} \quad (2a)$$

$$k_{\text{HNu}} = k_{\text{Nu}}' / K_a^{H-1} \quad (2b)$$

Kresge and coworkers presented convincing arguments that the addition of thiocyanate anion NCS^- to $\mathbf{p-H-1}^+$ is diffusion limited and that this reaction could be used as a clock for the slower reaction of solvent. Combining a value $k_{\text{Nu}}' = 5 \times 10^9 \text{ M}^{-1} \text{ s}^{-1}$, which is typical for diffusion-limited addition of nucleophiles to carbocations,¹⁴⁷ with $k_{\text{HNu}} = 4.5 \times 10^7 \text{ M}^{-2} \text{ s}^{-1}$ for acid-catalyzed addition of thiocyanate anion NCS^- (eq 2a) gives $K_a^{H-1} = 110 \text{ M}$ for deprotonation of $\mathbf{p-H-1}^+$.⁵² Substitution of $K_a^{H-1} = 110 \text{ M}$ and $k_H = 5.3 \times 10^4 \text{ M}^{-1} \text{ s}^{-1}$ into eq 2b gives $k_s' = 5.8 \times 10^6 \text{ M}^{-1} \text{ s}^{-1}$ for addition of water to $\mathbf{p-H-1}^+$. The rate constants for addition of water to $\mathbf{p-1}$, $\mathbf{p-H-1}^+$ and $\mathbf{p-Me-1}^+$ are summarized in Table 1.

11. O-Protonation of the Quinone Oxygen: Stability Effects

Scheme 40 shows a complete set of rate and equilibrium constants for addition of water to $\mathbf{p-H-1}^+$ and $\mathbf{p-1}$ and for deprotonation of $\mathbf{p-H-1}^+$ and $\mathbf{p-H-1-OH}$ - the phenol product of addition of water to $\mathbf{p-H-1}^+$. These rate and equilibrium constants (Table 2) were determined as follows.³

1. The Brønsted acidity constant $\text{p}K_a^{\text{P}} = 9.9$ for the stable product has been determined by direct measurement. The value of $\text{p}K_a^{\text{H-1}} = -2.0$ was determined as described above.³
2. A value of $\text{p}K_{\text{R}}^{\text{H-1}} = -\log(k_s/k_H) = -9.6 \pm 0.1$ for the Lewis acidity constant of $\mathbf{p-H-1}^+$ was calculated from $k_H = 1.5 \times 10^{-3} \text{ M}^{-1} \text{ s}^{-1}$ for acid-catalyzed cleavage of $\mathbf{p-H-1-OH}$ ³ and $k_s = 5.8 \times 10^6 \text{ s}^{-1}$ for nucleophilic addition of solvent water to $\mathbf{p-H-1}^+$.⁵²
3. A value of $\text{p}K_{\text{add}}^1 = -7.6$ for the 1,6-addition of water to $\mathbf{1}$ to give $\mathbf{p-H-1-OH}$ was calculated from the values of $\text{p}K_{\text{R}}^{\text{H-1}} = -9.6$ and $\text{p}K_a^{\text{H-1}} = -2.0$ [see above] for deprotonation of the phenolic oxygen of $\mathbf{p-H-1}^+$, according to eq 3.³
4. A value of $\text{p}K_{\text{R}}^1 = 2.3 \pm 0.1$ for the Lewis acidity constant of $\mathbf{p-1}$ was calculated from $\text{p}K_{\text{add}}^1 = -7.6$ and $\text{p}K_a^{\text{P}} = 9.9$ for deprotonation of the phenolic oxygen of $\mathbf{p-H-1-OH}$, according to eq 4.

These data show that protonation of the quinone oxygen of $\mathbf{p-1}$ to give $\mathbf{p-H-1}^+$ causes a 16 kcal/mol increase in the thermodynamic driving force for addition of water to the benzylic carbon (Scheme 41). By comparison, the value of $\text{p}K_{\text{R}} = -12.4$ for the Lewis acidity constant of the 4-methoxybenzyl carbocation $\mathbf{p-Me-1}^+$,³³ shows that *O*-methylation of $\mathbf{1}$ to give $\mathbf{p-Me-1}^+$ causes an even larger 20 kcal/mol increase in the driving force for water addition to the benzylic carbon. These results provide evidence that O-protonation of $\mathbf{p-1}$ is an imperfect model for O-alkylation. The smaller driving force for addition of water to $\mathbf{p-H-1}^+$ center reflects, at least in part, the stabilization of $\mathbf{p-H-1}^+$ by hydrogen bonding to water (Scheme 41). The are consistent with the formation of a hydrogen bond to water that has a covalent component and leads to a weakening in the ring O-H bond accompanied by a shift of electron-density from oxygen to the benzylic carbon.

$$pK_{\text{add}}^1 = pK_R^{H-1} - pK_a^{H-1} \quad (3)$$

$$pK_R^1 = pK_{\text{add}}^1 + pK_a^P \quad (4)$$

12. O-Alkylation and O-Protonation of the Quinone Methide Oxygen: Effect on Intrinsic Reaction Barriers

The kinetic barriers to organic reactions depend upon both the thermodynamic driving force to the reaction (Figure 3A) and the “intrinsic” barrier (Λ , Figure 3B) to the reaction in the absence of any driving force ($\Delta G^\circ = 0$).^{148,149} The effect of alkylation of the quinone oxygen of quinone methide **p-1** and of alkylation of a simple carbonyl carbon are compared in Scheme 42. Methylation of **p-1** to form **p-Me-1** results in a large 20 kcal/mol increase in the driving force for addition of solvent water to give the initial ionic adduct. By comparison, there is a smaller 1.7 kcal/mol change in the Marcus intrinsic reaction barrier.³ The Marcus intrinsic barrier for addition of water to **p-1** is smaller than for the addition of water to formaldehyde, a simple carbonyl electrophile (Scheme 42). It is interesting that alkylation of **p-1** and of acetaldehyde cause similar 1.7 kcal/mol and 2.2 kcal/mol, respectively, decreases in the intrinsic barrier for addition reactions of these oxygen nucleophiles.³

There is good evidence that an intrinsic barrier Λ for thermoneutral nucleophile addition to a resonance-stabilized carbocation is observed when the energetic cost of the loss of stabilizing resonance interactions at the transition state exceeds the compensating transition state stabilization resulting from partial carbon-nucleophile bond formation, so that there is an *imbalance* in the changes in these opposing interactions.^{150–152} It is well-known that these intrinsic barriers increase, with increasing carbocation stabilization by resonance.^{132,146} However, the data in Scheme 42 suggests that the change in Λ with thermodynamic driving force is small.

Nucleophile addition to a quinone methide is *formally* a Michael addition reaction.¹⁵³ However, an important difference between 1,6-addition of nucleophiles to *p*-quinone methides and conventional Michael addition reactions is the aromatization of the cyclohexadiene ring that accompanies this addition. The effect of aromatic ring formation on the thermodynamic driving force for 1,6-addition of water to **p-1** has been evaluated by comparing the thermodynamics for addition of water to **p-1** with that for the related 1,2-addition of water to formaldehyde (Scheme 43).¹³⁰

The net effect of this cyclohexadiene/phenyl ring insertion at the carbonyl group is to cause an increase in the overall equilibrium constant for the addition of solvent water, from $K_{\text{add}}^{\text{F}} = 2.3 \times 10^3$ for hydration of formaldehyde,¹⁵⁴ to $K_{\text{add}}^1 = 4.0 \times 10^7$ for hydration of the *p*-quinone methide **1**,³ so that $K_{\text{T}} = K_{\text{add}}^1 / K_{\text{add}}^{\text{F}} = 1.7 \times 10^4$ for transfer of the elements of water from formaldehyde hydrate to **1** (Scheme 43). We have proposed that the relatively small driving force of 6 kcal/mol for this transfer of water from $\text{CH}_2(\text{OH})_2$ to **1** represents the balance between larger opposing effects:³

1. The ca. 31 kcal greater stability of the reactant formaldehyde hydrate than of the product *p*-(hydroxymethyl)phenol **H-1-OH** due to the stronger single bonds to oxygen. This is a result of the 15 kcal/mol stabilizing interactions between the geminal oxygens at $\text{CH}_2(\text{OH})_2$,¹⁵⁵ and the weakening of the phenolic O-H bond at **H-1-OH** due to the ca. 16 kcal/mol stabilization of the alkoxy radical by the aromatic ring.³

2. The even larger ca. $(31 + 6) = 37$ kcal/mol driving force associated with the formal aromatic stabilization of the six-membered ring at the product **H-1-OH** than at the reactant **1**. It is interesting that this effect is very similar to the total aromatic stabilization of a phenyl ring, which has been estimated to lie between 30 and 36 kcal/mol.¹⁵⁶ This analysis suggests that the zwitterionic aromatic valence bond resonance structure (Scheme 38) makes a relatively small contribution of the structure of **p-1**. Similarly, the large difference in the basicity of **p-1** ($pK_a^{H-1} = -2.0$, Table 2) and the phenoxide anion (**p-1-OH**)⁻ provides strong evidence that the bonding to the quinone oxygen of **p-1** is similar to that for a carbonyl group.

13. O-Alkylation of the Quinone Methide Oxygen: Effect on Hammett Reaction Constants

Values of $\rho = 2.7$ ¹³⁸ and $\rho = 3.0$ ¹⁵⁷ have been determined for addition of water to *meta*-substituted 1-(4-methoxyphenyl)ethyl carbocations (**80a**, Scheme 44A) and 1-4-methoxybenzyl carbocations (**p-Me-1⁺-X**), respectively. The value of $\rho = 2.7$ for addition of water to **80a** is 36% that of the value of $\rho_{eq} = 7.6$, the slope of Hammett-type plots equilibrium constants for addition of water to **80a** to form the alcohol.¹³⁸ The reactions shown in Scheme 44A therefore proceed through a transition state in which there is a 36% change in the interaction between the *m*-substituent and positive charge at the benzylic carbon due to partial bond formation to the water nucleophile.

By contrast, two observations suggest that the addition of water to **o-1-m-X** (Scheme 44B) proceeds through a late, product-like transition state in which there is strong bonding between water and the quinone carbon and a large buildup of negative charge at the quinone oxygen.

1. The value of $\rho = 5.9$ ¹⁵⁸ determined for addition of water to **o-1-m-X** (Scheme 44B) is much larger than the values of $\rho = 2.7$ ¹³⁸ and $\rho = 3.0$ ¹⁵⁷ determined for addition of water to **80a**, and **p-Me-1⁺-X**, respectively.
2. The rate data for the reactions of **o-1-m-X** show a good fit to Hammett substituent constants σ^- developed using ionization of ring substituted phenols as a reference reaction.¹⁵⁹ This is consistent with a late transition state, that is stabilized by a resonance interaction between the phenoxide-like ring oxygen and resonance electron-withdrawing groups at the position *para* to the ring oxygen. It is interesting that the value of $\rho = 5.9$ for addition solvent to **o-1-m-X** is substantially greater than $\rho = 2.2$ for equilibrium deprotonation of phenols,¹⁵⁹ but we are unsure of the significance of this result.

14. Ortho-Quinone and Ortho-Thioquinone Methides

The pL-rate profiles (not shown) of rate constants k_{obs} for the disappearance of **o-1** in H₂O and D₂O also show good fit to eqs 1, now derived for Scheme 45, using values of $k_s = 230$ s⁻¹ (Table 1) and $k_H = 8.4 \times 10^5$ M⁻¹ s⁻¹ (X = O).⁵⁰ The value of $pK_a^{H-1} = -1.7$ for deprotonation of **oH-1⁺** was estimated as described above for **p-1**. The pL-rate profiles (not shown) of k_{obs} for the disappearance of *o*-thioquinone methide **81** in H₂O and D₂O also show good fit to eq 1 using values of $k_s = 1.2 \times 10^5$ s⁻¹ (Table 1) and $k_H = 7.0 \times 10^4$ M⁻¹ s⁻¹ (Table 1), where k_s is the first order rate constant for addition of solvent to **81** and k_H is the second order rate constant for catalysis of solvent addition by hydronium ion (Scheme 45, X = S).⁵⁸ The pL rate profiles for reaction of **81** are linear in [L⁺] down to pL = -3. This shows that the $pK_a < -3$ for loss of a proton from the strongly acidic S-protonated *o*-thioquinone methide.

The *ca* 50,000-fold difference in the values of k_s for addition of water to **81** and **p-1** is perhaps not surprising, given the complexity of the other known effects of sulfur for oxygen substitutions on the rate and equilibrium constants for nucleophile addition to carbocations.^{130,160} These results show that *both* the change in the position of the aromatic substituents from *para* to *ortho* and the substitution of sulfur for oxygen cause in a increase in the *electrophilic* zwitterionic resonance form to the resonance hybrid structure. We suggest that this increase in quinone methide electrophilic reactivity reflects the increasing contribution of the reactive zwitterionic resonance form on moving from **p-1** to **o-1** to **81** (Scheme 46).

The contribution of the zwitterionic valence bond resonance form to the overall structures should depend upon the balance between stabilization of this structure from aromaticity and the energetic cost of localization of charge at carbon oxygen. We suggest that the cost of charge localization is lower for **o-1** than **p-1** because of the greater stabilizing electrostatic interactions between the closely spaced charges at the *ortho*-quinone carbon and oxygen. Sulfur is more polarizable than oxygen and provides more effective stabilization of both positive and negative charge. This is shown by the greater acidity of thiophenol ($pK_a = 7$) than phenol ($pK_a = 10$).¹⁶¹ The high polarizability of sulfur will favor the *formally* reactive zwitterionic resonance form of *o*-thioquinone methide compared to the *o*-quinone methide (Scheme 46).

The lower reactivity of the *o*-thioquinone methide **81** ($7.0 \times 10^4 \text{ M}^{-1} \text{ s}^{-1}$) compared with the **o-1** ($8.4 \times 10^5 \text{ M}^{-1} \text{ s}^{-1}$) in acidic solution contrasts with the much higher reactivity of **81** at neutral pH (Table 1). This may represent the balance between the smaller concentration of the protonated thioquinone methide compared with protonated **o-1** due to the weaker basicity of *o*-S ($pK_a < -3$, Table 1) compared with *o*-S ($pK_a < -1.7$), and the presumably greater intrinsic reactivity of **H-81**⁺.⁵⁸ However, the observed effects of sulfur for oxygen substitution on carbocation reactivity have in the past proven very difficult to rationalize,^{130,160} and in the present case are probably not fully understood.

Very different solvent deuterium isotope effects (SDIE) of $(k_H)/(k_D) = 0.42$ and 1.66, respectively, are observed for acid-catalyzed addition of solvent to **o-1** and **81**.^{50,58} The inverse SDIE for hydration of **o-1** is consistent with initial fast and reversible protonation of substrate followed by rate determining addition of solvent to the protonated benzylic carbocation **o-H-1**⁺. The normal primary SDIE on acid-catalyzed hydration of **81** is consistent with a change in mechanism from stepwise, for acid-catalyzed addition of water **o-1**,⁵⁰ to concerted for the acid-catalyzed reaction of **81**, where the addition of water and hydron occur at a single reaction stage (k_{con} , Scheme 45).

These data could also be rationalized if there were a change in the rate-determining step for a stepwise reaction, from k_s' for acid-catalyzed addition of solvent to **o-1** to k_1 for the reaction of **81**. However, it is unlikely that k_1 will be rate determining for the stepwise addition to **81**. This would require $k_s' > k_{-1}$ for Scheme 47. A value of $k_{-1} > 10^{10} \text{ s}^{-1}$ is expected for the strongly favorable deprotonation of **H-81**⁺ by water,¹⁶² and there is evidence for a significant barrier to k_s' for addition of water to $-\text{SR}$ substituted benzylic carbocations. For example, a value of $k_s' = 5 \times 10^7 \text{ s}^{-1}$ has determined for addition of an aqueous solvent to the 1-(4-thiomethyl)-1-phenylethyl carbocation ($R = \text{SMe}$). The concerted mechanism is favored because it avoids formation of the unstable acidic intermediate **H-81**⁺. It is possible, but not proven, that the concerted mechanism is enforced by the absence of a vibrational barrier to the step k_{-1} for deprotonation of this very strongly acid reaction intermediate by water.^{163,164}

15. The di- α -CF₃-Substituted Quinone Methide

The quinone methide **48** was generated by nucleophilic aromatic substitution of water at **Me-48**⁺ as shown in Scheme 23,⁸⁹ and its reaction with solvent and added nucleophiles studied in water and in 50/50 (v/v) H₂O/trifluoroethanol at 25 °C.^{4,67,89,91} The addition of a pair of strongly electron-deficient α -CF₃ groups to the parent unsubstituted *para*-quinone methide **p-1** should increase the electrophilic reactivity of the quinone carbon due to a polar effect. Therefore, the observation that the 18 minute lifetime for **48** in water⁴ is much longer than the *ca* 0.5 second lifetime for **1** in the same solvent therefore shows that these substituent effects cannot be understood by a simple consideration of polar effects.¹³² There is an unusually large intrinsic barrier for addition of nucleophiles to **48**, so that both the electrophile and its nucleophile adducts show an unusual kinetic stability relative to other carbocations. This has allowed for an examination of previously inaccessible carbocation-nucleophile addition reactions, that has provided unique insight into their structure-reactivity relationships.

A complete description of these substituent effects is obtained by comparing the rate and equilibrium constants for the addition of HBr to **48** (Figure 4A)⁹¹ and to **p-1** (Figure 4B)⁵² and of the derived free energy reaction profiles shown in Figure 4.⁵² The 1.7 kcal/mol larger driving force for addition of HBr to **48** shows that the electron-deficient α -CF₃ groups cause only a modest destabilization of the electrophilic quinone methide carbon. This reflects: (a) The large contribution of resonance structure B (Scheme 48) where the benzylic carbon is neutral. (b) The compensating destabilization of the bromide adduct **H-48-Br** by steric/electrostatic interactions between the α -Br and α -CF₃ groups.^{89,91} The most striking feature of these free energy profiles is the much larger kinetic barrier for nucleophile addition to **48**, compared to addition to **p-1** and for the cleavage of **H-48-Br**, the nucleophile adduct to **48**. This reflects the 9 kcal/mol large Marcus intrinsic barrier to nucleophile addition to **48** compared with addition to **p-1**.^{52,132}

The intrinsic barriers to both addition of nucleophiles to unstable electrophiles and the protonation of unstable carbanions are known to increase with increasing resonance delocalization of charge onto compatible substituents.^{129,132,133,137,139} The very large intrinsic barriers for nucleophile additions to **48** are consistent with the notion that this electrophile is an extreme example of a benzylic-type carbocation, where extensive delocalization of charge away from the quinone carbon is *driven* by the resulting relief of destabilizing polar interactions between the electrophilic carbon and the electron-deficient α -CF₃ groups. Consequently, the neutral, non-aromatic resonance form B makes a exceptionally large contribution to the structure of **48** (Scheme 48).

Two pathways are observed for nucleophile addition to **48** in water (Scheme 49). (i) Uncatalyzed nucleophile addition to form the oxygen anion ⁻**48** that undergoes rapid protonation. (ii) Specific-acid catalyzed nucleophile addition. The solvent deuterium isotope effects on the specific-acid catalyzed addition of solvent and bromide anion to **48** are $k_H/k_D = 0.68$ and 1.0, respectively for reactions in 50/50 (v/v) water trifluoroethanol,⁶⁷ but a smaller SDIE of $k_H/k_D = 0.41$ is observed for the specific-acid catalyzed addition of an aqueous solvent to **1**.⁵² The larger SDIE for acid-catalyzed addition of Br⁻ to **48** is consistent with a concerted reaction mechanism, in which protonation of oxygen and carbon-bromine bond formation occur in a single step with a rate constant k_{HBr} (Scheme 49).

Second-order rate constants k_Y (Scheme 49) were determined for addition of a wide range of nucleophiles to **48**.⁴ Figure 5 shows the linear correlation between values of $\log k_Y$ and the Ritchie nucleophilicity parameter N_+ with a slope of $s = 0.92$ that is essentially the same as

the electrophile independent values of $s = 1.0$ determined for nucleophile addition to highly resonance stabilized carbocations, such as ring-substituted triarylmethyl carbocations (Scheme 48).^{5,165} These data show that, by the criterion of its chemical reactivity, **1** behaves as a highly resonance stabilized carbocation, similar to the ring-substituted triarylmethyl carbocations used to establish the N_+ scale. It was possible to obtain second-order rate constants for addition of weak nucleophiles to **48** (open symbols, Figure 5) because of the unusually high stability of the product nucleophile adducts in aqueous acidic solution. This allowed for the estimation of previously unavailable N_+ values for these weak nucleophiles, by making that assumption that the rate constants for their addition to **48** lie on the linear correlation defined by other Ritchie electrophiles (Figure 5).⁴

Table 3 compares the thermodynamic driving force ΔG° , calculated from the equilibrium constant K_{add} (Scheme 50) and the derived Marcus intrinsic reaction barriers for reversible addition of nucleophiles Y^- to **48** and to the triphenylmethyl carbocation (Ph_3C^+).⁴ There are nearly constant differences between the values for the thermodynamic driving force for addition of nucleophiles to **48** and to Ph_3C^+ [$(\Delta G^\circ(\mathbf{48}) - \Delta G^\circ(\text{PhC}^+)) = 8.4$ kcal/mole] and of Λ [$\Lambda(\mathbf{48}) - \Lambda(\text{PhC}^+) = 5.2$ kcal/mol] for the addition of chloride, bromide, and acetate ions to **1** and Ph_3C^+ .⁴ The ca. 8 kcal/mol more unfavorable change in ΔG° for nucleophile addition to **48** than to Ph_3C^+ shows that resonance electron donation to the benzylic carbon of **1** is more stabilizing than the corresponding electron donation from the three phenyl rings at Ph_3C^+ . The ca. 5 kcal/mol larger intrinsic barrier for nucleophile addition to **48** is consistent with the notion that the effect of this larger carbocation stabilization by resonance is to make carbocation-nucleophile addition more difficult in both a thermodynamic and a kinetic sense.^{89,90,92,129,132,160} The almost constant relative values of ΔG° and Λ for the addition of different nucleophiles to **48** and to Ph_3C^+ is striking and requires that variations in the structure of the nucleophile bring about the same change in the stability of the transition state and products for the reaction of these two electrophiles. This suggests a similar development of nucleophile-electrophile bonding interactions at these transition states.

Rate constants k_Y ($\text{M}^{-1} \text{s}^{-1}$) and k_{solV} (s^{-1}) for the reversible addition of methanethiol to **48** and the overall reaction equilibrium constant (Scheme 51) have been reported.⁸³ It was shown that the transition state for addition of RSH to **1** is stabilized by electron-donating alkyl groups and by substitution of an electron donating methyl group for hydrogen at CH_3SH . These data are consistent with a relatively late, product like transition state for nucleophile addition. By contrast, the dimethylsulfide adduct $^-\mathbf{48}\text{-SMe}_2^+$ is strongly destabilized by interactions between the cationic sulfonium ion and electron-withdrawing $\alpha\text{-CF}_3$ groups, but there is relatively little destabilization of the transition state for addition of Me_2S to **48** from interactions between the developing cationic center at the sulfur nucleophile and the electron-withdrawing $\alpha\text{-CF}_3$ groups.⁸³ In other words, the weak development at the transition state of the strongly product destabilizing steric interactions with the incoming nucleophile, is consistent with an early transition state for addition of Me_2S . The results suggest that C-S bonding interactions at the transition state for addition of Me_2S to **48** develop at a relatively long distance, and that steric/electrostatic interactions which destabilize the product nucleophile adduct only become significant, after the transition state has been traversed on the reaction coordinate. The results are consistent with the notion that Me_2S is a large, "soft", polarizable nucleophile, similar to I^- and RS^- with the property that it provides electrons to form a partial bond with the electrophilic carbon of **48** from a larger distance than smaller, "harder" nucleophilic atoms.¹⁶⁶

Acknowledgments

The work from our laboratory discussed in the review was generously supported by GM 39754 from the National Institutes of Health.

References

1. Capponi M, Gut IG, Hellrung B, Persy G, Wirz J. *Can J Chem.* 1999; 77:605–613.
2. Gomez I, Rodríguez E, Reguero M. *J Mol Struct.* 2006; 767:11–18.
3. Toteva MM, Moran M, Amyes TL, Richard JP. *J Am Chem Soc.* 2003; 125:8814–8819. [PubMed: 12862476]
4. Richard JP, Toteva MM, Crugeiras J. *J Am Chem Soc.* 2000; 122:1664–1674.
5. Ritchie CD. *Acc Chem Res.* 1972; 5:348–54.
6. Richter D, Hampel N, Singer T, Ofial AR, Mayr H. *Eur J Org Chem.* 2009:3203–3211.
7. Selenski C, Pettus TR. *J Org Chem.* 2004; 69:9196–203. [PubMed: 15609955] Marsini MA, Huang Y, Lindsey CC, Wu K-L, Pettus TRR. *Org Lett.* 2008; 10:1477–1480. [PubMed: 18336038]
8. Goodman JL, Peters KS, Lahti PM, Berson JA. *J Am Chem Soc.* 1985; 107:276–277. Khan MI, Goodman JL. *J Am Chem Soc.* 1994; 116:10342–10343.
9. Rokita, SE. *Quinone Methides.* John Wiley & Sons; Hoboken, NJ: 2009.
10. McClelland RA. *Tetrahedron.* 1996; 52:6823–6858.
11. Wan P, Barker B, Diao L, Fisher M, Shi Y, Yang C. *Can J Chem.* 1996; 74:465–475.
12. Wan P, Brousmiche DW, Chen CZ, Cole J, Lukeman M, Xu M. *Pure Appl Chem.* 2001; 73:529–534.
13. Krull IS, Arnold DR. *Tetrahedron Lett.* 1969:1247.
14. Chapman OL, McIntosh CL. *J Chem Soc, Chem Commun.* 1971:383–384.
15. Padwa A, Dehm D, Oine T, Lee GA. *J Chem Soc.* 1975; 97:1837–1845.
16. Creed D. *J Chem Soc, Chem Commun.* 1976:121–122.
17. Jacqmin G, Nasielski J, Billy G, Remy M. *Tetrahedron Lett.* 1973:3655–3656.
18. Padwa A, Lee G. *J Chem Soc, Chem Commun.* 1976:795–796.
19. Leary G. *J Chem Soc, Perkin Trans 2.* 1970:640–642.
20. Hemmingson JA, Leary G. *J Chem Soc, Perkin Trans 2.* 1975:1584–1587.
21. (a) Angle SR, Turnbull KD. *J Am Chem Soc.* 1990; 112:3698–3670. (b) Angle SR, Turnbull KD. *J Org Chem.* 1993; 58:5350–5369.
22. Wan P, Culshaw S, Yates K. *J Chem Soc.* 1982; 104:2509–2515.
23. Kirmse W, Guth M, Steenken S. *J Am Chem Soc.* 1996; 118:10838–10849.
24. Bartl J, Steenken S, Mayr H. *J Am Chem Soc.* 1991; 113:7710–7716.
25. Kalaneropoulos P, Yates K. *J Chem Soc.* 1986; 108:6290–6295.
26. Kasha M. *J Chem Soc, Faraday Trans 2.* 1986; 82:2379–2392.
27. Lukeman M, Wan P. *J Chem Soc, Chem Commun.* 2001:1004–1005.
28. Lukeman M, Wan P. *J Am Chem Soc.* 2002; 124:9458–9454. [PubMed: 12167041]
29. Shi Y, Wan P. *J Chem Soc, Chem Commun.* 1995:1217–1218.
30. Wan P, Chak B. *J Chem Soc, Perkin Trans 2.* 1986:1751–1756.
31. Wan P. *J Org Chem.* 1985; 50:2583–2585.
32. Wan P, Yates K, Boyd MK. *J Org Chem.* 1985; 50:881–1886.
33. Diao L, Yang C, Wan P. *J Am Chem Soc.* 1995; 117:5369–5370.
34. Lewis TW, Curtin DY, Paul IC. *J Am Chem Soc.* 1979; 101:5717–5725.
35. Hamai S, Kokubun H. *Bull Chem Soc Jpn.* 1974; 47:2085–2088.
36. Seiler P, Wirz J. *Helv Chim Acta.* 1972; 55:2694–2712.
37. Gao J, Li N, Freindorf M. *J Am Chem Soc.* 1996; 118:4912–4913.
38. Foster KL, Baker S, Brousmiche DW, Wan P. *J Photochem Photobiol A.* 1999; 129:157–163.

39. McClelland RA, Moriarty MM, Chevalier JM. *J Chem Soc, Perkin Trans 2*. 2001;2235–2236.
40. Brousmiche D, Wan P. *J Chem Soc, Chem Commun*. 1998
41. Brousmiche DW, Wan P. *J Photochem Photobiol A*. 2002; 149:71–81.
42. (a) Richter SN, Maggi S, Mels SC, Palumbo M, Freccero M. *J Am Chem Soc*. 2004; 126:13973–13979. [PubMed: 15506758] (b) Chatterjee M, Rokita SE. *J Am Chem Soc*. 1994; 116:1690–1697.
43. Colloredo-Mels S, Doria F, Verga D, Freccero M. *J Org Chem*. 2006; 71:3889–3895. [PubMed: 16674065]
44. McClelland RA, Mathivanan N, Steenken S. *J Am Chem Soc*. 1990; 112:4857–4861.
45. Amyes TL, Richard JP, Novak M. *J Am Chem Soc*. 1992; 114:8032–41.
46. Allen AD, Tidwell TT. *Chem Rev*. 2001; 101:1333–1348. [PubMed: 11710224]
47. Mecklenburg SL, Hilinski EF. *J Am Chem Soc*. 1989; 111:5471–5472.
48. Wan P, Krogh E. *J Am Chem Soc*. 1989; 111:4887–4895.
49. Fisher M, Shi Y, Zhao B-p, Snieckus V, Wan P. *Can J Chem*. 1999; 77:868–874.
50. Chiang Y, Kresge AJ, Zhu Y. *J Am Chem Soc*. 2001; 123:8089–8094. [PubMed: 11506565]
51. Chiang Y, Kresge AJ, Zhu Y. *J Am Chem Soc*. 2000; 122:9854–9855.
52. Chiang Y, Kresge AJ, Zhu Y. *J Am Chem Soc*. 2002; 124:6349–6356. [PubMed: 12033864]
53. Chiang Y, Kresge AJ, Zhu Y. *J Am Chem Soc*. 2002; 124:717–722. [PubMed: 11804503]
54. Chiang Y, Kresge AJ, Zhu Y. *Photochem Photobiol Sci*. 2002; 1:67–70. [PubMed: 12659151]
55. Chiang Y, Kresge AJ, Zhu Y. *Phys Chem Chem Phys*. 2003; 5:1039–1042.
56. Chiang Y, Kresge AJ. *Org Biomol Chem*. 2004; 2:1090–1092. [PubMed: 15034634]
57. Chiang Y, Kresge AJ, Onyido I, Richard JP, Wan P, Xu M. *Chem Commun*. 2005:4231–4233.
58. Chiang Y, Kresge AJ, Sadovski O, Zhan H-Q. *J Org Chem*. 2005; 70:1643–1646. [PubMed: 15730283]
59. Chiang Y, Kresge AJ, Hellrung B, Schunemann P, Wirz J. *Helv Chim Acta*. 1997; 80:1106–1121.
60. Zhang K, Corrie JET, Munasinghe VRN, Wan P. *J Am Chem Soc*. 1999; 121:5625–5632.
61. (a) Huang CG, Shukla D, Wan P. *J Org Chem*. 1991; 56:5437–5442. (b) Huang C-G, Wan P. *J Org Chem*. 1991; 56:4846–4853.
62. Arumugam S, Popik VV. *J Am Chem Soc*. 2009; 131:11892–11899. [PubMed: 19650661]
63. Guthrie RD, Jencks WP. *Acc Chem Res*. 1989; 22:343–349.
64. Richard JP, Jencks WP. *J Am Chem Soc*. 1984; 106:1383–1396.
65. Amyes TL, Richard JP. *J Am Chem Soc*. 1991; 113:8960–8961.
66. Hine, J. *Structural Effects on Equilibria in Organic Chemistry*. Wiley; New York: 1975.
67. Richard JP. *J Am Chem Soc*. 1991; 113:4588–95.
68. Filar LJ, Winstein S. *Tetrahedron Lett*. 1960; 25:9–16.
69. Sheppard WA. *J Org Chem*. 1968; 33:3297–3306.
70. Murray JJ. *J Org Chem*. 1968; 33:3306–3308.
71. Mare, PBDdl; Newman, PA. *J Chem Soc, Perkin Trans 2*. 1984
72. Skibo EA. *J Org Chem*. 1992; 57:5874–5878.
73. Skibo EB. *J Org Chem*. 1986; 51:522–527.
74. Pospisek J, Pisova M, Soucek M, Exner O. *Coll Czech Chem Com*. 1975; 40:2093–2098.
75. Modica E, Zanaletti R, Freccero M, Mella M. *J Org Chem*. 2001; 66:41–52. [PubMed: 11429928]
76. (a) Dyer RG, Turnbull KD. *J Org Chem*. 1999; 64:7988–7995. (b) Myers JK, Widlanski TS. *Science*. 1993; 262:1451–1453. [PubMed: 8248785]
77. Myers JK, Cohen JD, Widlanski TS. *J Am Chem Soc*. 1995; 117:11049–11054.
78. Wang Q, Dechert U, Jirik F, Withers SG. *Biochem Biophys Res Comm*. 1994; 200:577–83. [PubMed: 8166732]
79. Stowell JK, Widlanski TS, Kutateladze TG, Raines RT. *J Org Chem*. 1995; 60:6930–6936.
80. Abeles RH, Maycock AL. *Acc Chem Res*. 1976; 9:313–319.
81. Betley JR, Cesaro-Tadic S, Mekhafia A, Rickard JH, Denham H, Partridge LJ, Pluckthun A, Blackburn GM. *Angew Chem, Int Ed*. 2002; 41:775–777.

82. Liu Y, Lien I-FF, Ruttgaizer S, Dove P, Taylor SD. *Org Lett.* 2004; 6:209–212. [PubMed: 14723530]
83. Ahmed V, Liu Y, Taylor SD. *Chembiochem.* 2009; 10:1457–1461. [PubMed: 19466699]
84. Pande P, Shearer J, Yang J, Greenberg WA, Rokita SE. *J Am Chem Soc.* 1999; 121:6773–6779.
85. Velkuyzen WF, Shallop AJ, Jones RA, Rokita SE. *J Am Chem Soc.* 2001; 123:11126–11132. [PubMed: 11697955]
86. Zeng Q, Rokita SE. *J Org Chem.* 1996; 61:9080–9081.
87. Allen AD, Kanagasabapathy VM, Tidwell TT. *J Am Chem Soc.* 1986; 108:3470–4.
88. Richard JP. *J Am Chem Soc.* 1989; 111:6735–44.
89. Richard JP, Amyes TL, Bei L, Stubblefield V. *J Am Chem Soc.* 1990; 112:9513–19.
90. Richard JP. *J Am Chem Soc.* 1989; 111:1455–1465.
91. Toteva MM, Richard JP. *J Am Chem Soc.* 2000; 122:11073–11083.
92. McClelland RA, Cozens FL, Steenken S, Amyes TL, Richard JP. *J Chem Soc, Perkin Trans 2.* 1993:1717–22.
93. Cook CD, Nash NG, Flanagan HR. *J Am Chem Soc.* 1955; 77:1783–1784.
94. Stebbins R, Sicilio F. *Tetrahedron.* 1970; 26:291–297.
95. (a) Cook CD, Norcross BE. *J Am Chem Soc.* 1956; 78:3797–3799. (b) Dyall LK, Winstein S. *J Am Chem Soc.* 1972; 94:2196–2199.
96. Angle SR, Ranier JD. *J Org Chem.* 1992; 57:6883–6890.
97. Angle SR, Arnaiz DO, Boyce JP, Frutos RP, Louie MS, Mattson-Arnaiz HL, Rainier JD, Turnbull KD, Yang W. *J Org Chem.* 1994; 59:6322–37.
98. Zhou Q, Turnbull KD. *J Org Chem.* 2000; 65:2022–2029. [PubMed: 10774022]
99. Angle SR, Yang W. *J Org Chem.* 1992; 57:1092–1097.
100. Angle SR, Rainier JD, Woytowicz C. *J Org Chem.* 1997; 62:5884–5892.
101. Sugumaran M, Dali H, Semensi V. *Bioorg Chem.* 1990; 18:144–153.
102. Crescenzi O, Costantini C, Protà G. *Tetrahedron Lett.* 1990; 31:6095–6096.
103. Tomasz M. *Chem & Biol.* 1995:575–579. [PubMed: 9383461]
104. Gaudiano G, Frigerio M, Sangsurasak C, Bravo P, Koch TH. *J Am Chem Soc.* 1992; 114:5546–53.
105. Moore HW. *Science.* 1977; 197:527–532. [PubMed: 877572]
106. O’Shea K, Fox MA. *J Am Chem Soc.* 1991; 113:611–615.
107. Sartorelli AC, Hodnick WF, Belcourt MF, Tomasz M, Haffty B, Fischer JJ, Rockwell S. *Oncol Res.* 1994; 6:501–8. [PubMed: 7620218]
108. Belcourt MF, Hodnick WF, Rockwell S, Sartorelli AC. *J Biol Chem.* 1998; 273:8875–81. [PubMed: 9535868]
109. McGuinness BF, Lipman R, Goldstein J, Nakanishi K, Tomasz M. *Biochemistry.* 1991; 30:6444–6453. [PubMed: 1905153]
110. Hong HP, Kohn H. *J Am Chem Soc.* 1991; 113:4634–4644.
111. McClelland RA, Lam K. *J Am Chem Soc.* 1985; 107:5182–5186.
112. Ouyang A, Skibo EB. *J Org Chem.* 1998; 63:1893–1900.
113. Khdour O, Ouyang A, Skibo EB. *J Org Chem.* 2006; 71:5855–5863. [PubMed: 16872163]
114. Kleyer DL, Koch TH. *J Am Chem Soc.* 1984; 106:2380–2387.
115. Gaudiano G, Frigerio M, Bravo P, Koch TH. *J Am Chem Soc.* 1992; 114:3107–3113.
116. Fisher J, Ramakrishnan K, Becvar JE. *Biochemistry.* 1983; 22:1347–1355. [PubMed: 6573203]
117. Bird DM, Gaudiano G, Koch TH. *J Am Chem Soc.* 1991; 113:308–315.
118. Gaudiano G, Frigerio M, Bravo P, Koch TH. *J Am Chem Soc.* 1990; 112:6704–6709.
119. Taatjes DJ, Gaudiano G, Resing K, Koch TH. *J Med Chem.* 1996; 39:4135–4138. [PubMed: 8863788]
120. Taatjes DJ, Gaudiano G, Resing K, Koch TH. *J Med Chem.* 1997; 40:1276–1286. [PubMed: 9111302]

121. Boldt M, Gaudiano G, Koch TH. *J Org Chem*. 1987; 52:2146–2153.
122. Chapman OL, McIntosh CL. *Journal of the Chemical Society [Section] D: Chemical Communications*. 1971:771.
123. Paul GC, Gajewski JJ. *J Org Chem*. 1993; 58:5060–5062.
124. Dorrestijn E, Pugin R, Nogales MVC, Mulder P. *J Org Chem*. 1997; 62:4804–4810.
125. Taing M, Moore HW. *J Org Chem*. 1996; 61:329–40.
126. Karabelas K, Moore HW. *J Am Chem Soc*. 1990; 112:5372–5373.
127. Rabin O, Vigalok A, Milstein D. *J Am Chem Soc*. 1998; 120:7119–7120.
128. Amyes TL, Richard JP. *J Am Chem Soc*. 1990; 112:9507–9512. [PubMed: 24074455]
129. Amyes TL, Stevens IW, Richard JP. *J Org Chem*. 1993; 58:6057–6066.
130. Richard JP. *Tetrahedron*. 1995; 51:1535–1573.
131. Richard JP, Amyes TL, Rice DJ. *J Am Chem Soc*. 1993; 115:2523–2524.
132. Richard JP, Amyes TL, Toteva MM. *Acc Chem Res*. 2001; 34:981–988. [PubMed: 11747416]
133. Richard JP, Amyes TL, Williams KB. *Pure Appl Chem*. 1998; 70:2007–2014.
134. Richard JP, Jagannadham V, Amyes TL, Mishima M, Tsuno Y. *J Am Chem Soc*. 1994; 116:6706–6712.
135. Richard JP, Jencks WP. *J Am Chem Soc*. 1982; 104:4689–4691.
136. Richard JP, Jencks WP. *J Am Chem Soc*. 1984; 106:1373–1383.
137. Richard JP, Lin S-S, Buccigross JM, Amyes TL. *J Am Chem Soc*. 1996; 118:12603–12613.
138. Richard JP, Rothenberg ME, Jencks WP. *J Am Chem Soc*. 1984; 106:1361–1372.
139. Richard JP, Williams KB, Amyes TL. *J Am Chem Soc*. 1999; 121:8403–8404.
140. Toteva MM, Richard JP. *J Am Chem Soc*. 2002; 124:9798–9805. [PubMed: 12175239]
141. Richard JP, Williams KB. *J Am Chem Soc*. 2007; 129:6952–6961. [PubMed: 17488079]
142. Tsang W-Y, Richard JP. *J Am Chem Soc*. 2009; 131:13952–13962. [PubMed: 19788330]
143. Richard JP, Jencks WP. *J Am Chem Soc*. 1984; 106:1396–1401.
144. Richard JP. *Adv Carbocation Chem*. 1989; 1:122–169.
145. Richard JP, Amyes TL, Toteva MM, Tsuji Y. *Adv Phys Org Chem*. 2004; 39:1–26.
146. Richard JP, Amyes TL, Lin SS, O'Donoghue AC, Toteva MM, Tsuji Y, Williams KB. *Adv Phys Org Chem*. 2000; 35:67–115.
147. McClelland RA, Kanagasabapathy VM, Banait NS, Steenken S. *J Am Chem Soc*. 1991; 113:1009–14.
148. Marcus RA. *J Am Chem Soc*. 1969; 91:7224–7225.
149. Marcus RA. *J Phys Chem*. 1968; 72:891–899.
150. Bernasconi CF. *Acc Chem Res*. 1992; 25:9–16.
151. Bernasconi CF. *Adv Phys Org Chem*. 1992; 27:119–238.
152. Bernasconi CF. *Acc Chem Res*. 1987; 20:301–308.
153. Valentin CD, Freccero M, Zanaletti R, Sarzi-Amade M. *J Am Chem Soc*. 2001; 123
154. Funderburk LH, Aldwin L, Jencks WP. *J Am Chem Soc*. 1978; 100:5444–5459.
155. Benson SW. *Angew Chem, Int Ed*. 1978; 17:812–819.
156. Schleyer, PvR; Manoharan, M.; Jiao, H.; Stahl, F. *Org Lett*. 2001; 3:3643–3646. [PubMed: 11700102]
157. Yeary, P. University of Kentucky. 1993.
158. Weinert EE, Dondi R, Colloredo-Melz S, Frankenfield KN, Mitchell CH, Freccero M, Rokita SE. *J Am Chem Soc*. 2006; 128:11940–11947. [PubMed: 16953635]
159. Hammett, LP. *Physical Organic Chemistry*. McGraw Hill; New York: 1940.
160. Jagannadham V, Amyes TL, Richard JP. *J Am Chem Soc*. 1993; 115:8465–8466.
161. Jencks, WP.; Regenstein, J. *Handbook of Biochemistry and Molecular Biology (Physical and Chemical Data)*. 3. Fasman, GD., editor. Vol. 1. CRC Press; Cleveland, OH: 1976. p. 305-351.
162. Eigen M. *Angew Chem, Int Ed*. 1964; 3:1–72.
163. Jencks WP. *Chem Soc Rev*. 1981; 10:345–375.

164. Jencks WP. *Acc Chem Res.* 1980; 13:161–9.
165. Ritchie CD. *Can J Chem.* 1986; 64:2239–50.
166. Gray CH, Coward JK, Schowen KB, Schowen RL. *J Am Chem Soc.* 1979; 101:4351–4358.

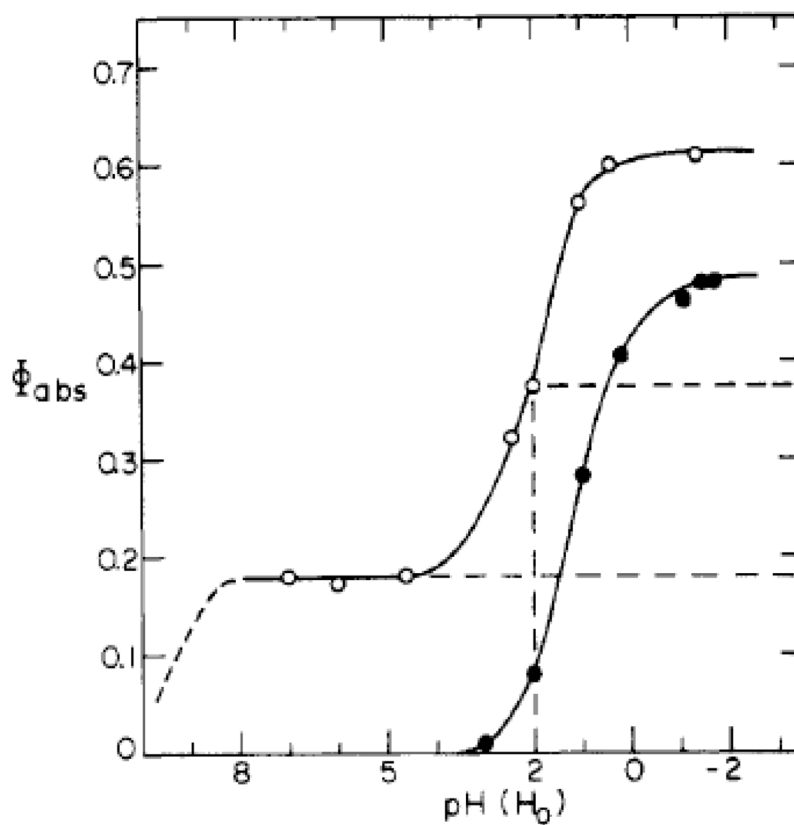


Figure 1. The pH profile for absolute quantum yields (Φ_{abs}) for the photohydration reaction of *o*-hydroxystyrene (open circles) and *p*-hydroxystyrene (closed circles) [Reprinted with permission of the American Chemical Society from Ref. 25].

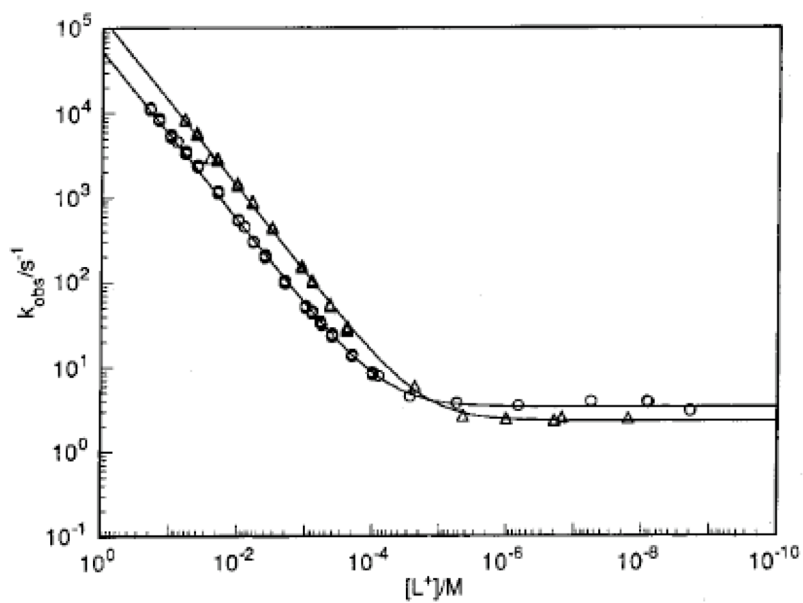


Figure 2. The pL rate profiles of the observed first-order rate constants k_{obs} for addition of solvent to *p*-**1** in H₂O (○) and in D₂O (△) at 25 °C. [Reprinted with permission of the American Chemical Society from Ref. 52].

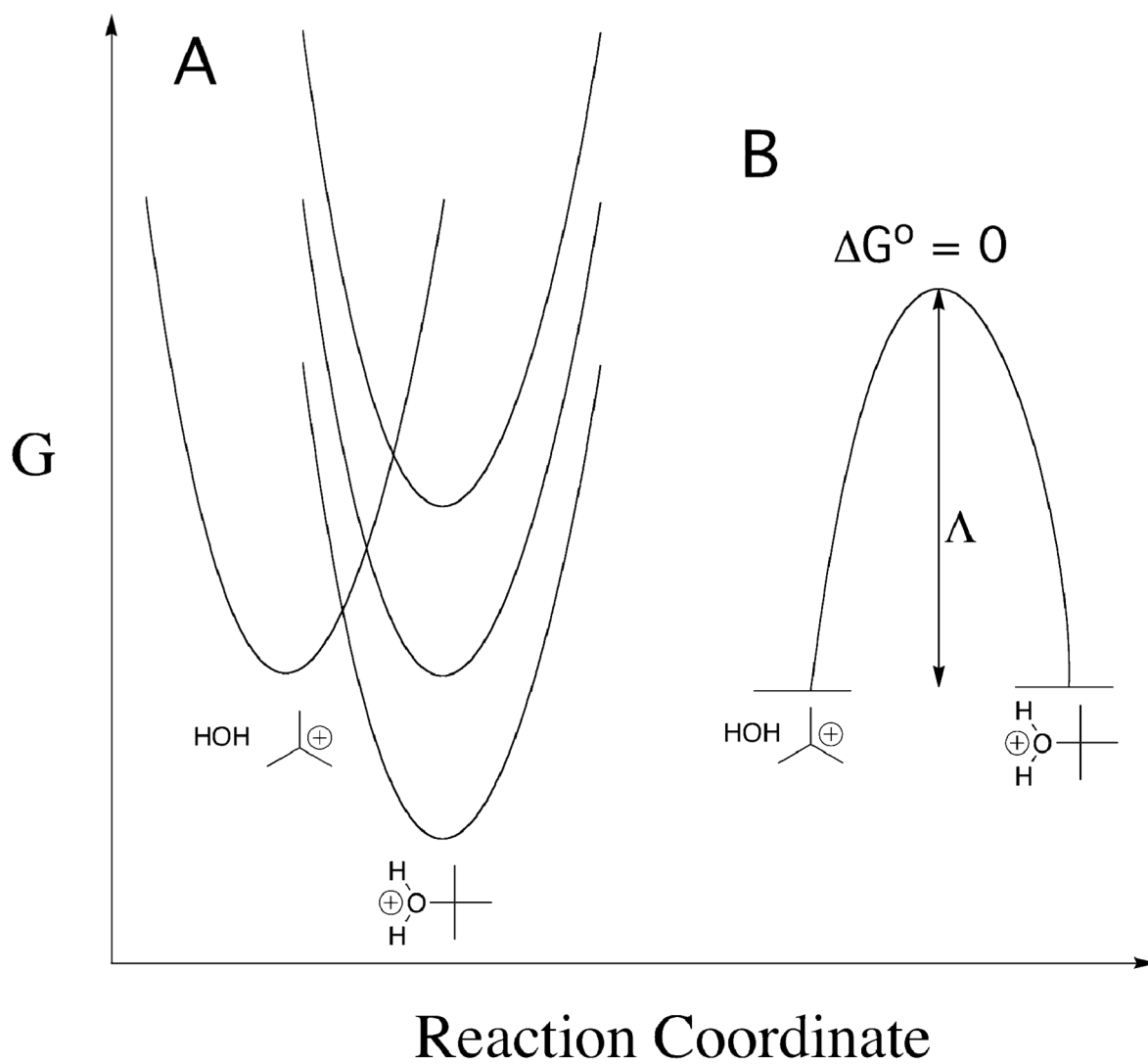


Figure 3.

(A) Free energy reaction profiles, constructed from intersecting parabolas, for addition of water to a simple carbocation which show the change in reaction barrier with changing reaction driving force. (B) Free energy profile for thermoneutral addition of water to a carbocation for which the observed activation barrier is equal to the intrinsic barrier Λ .

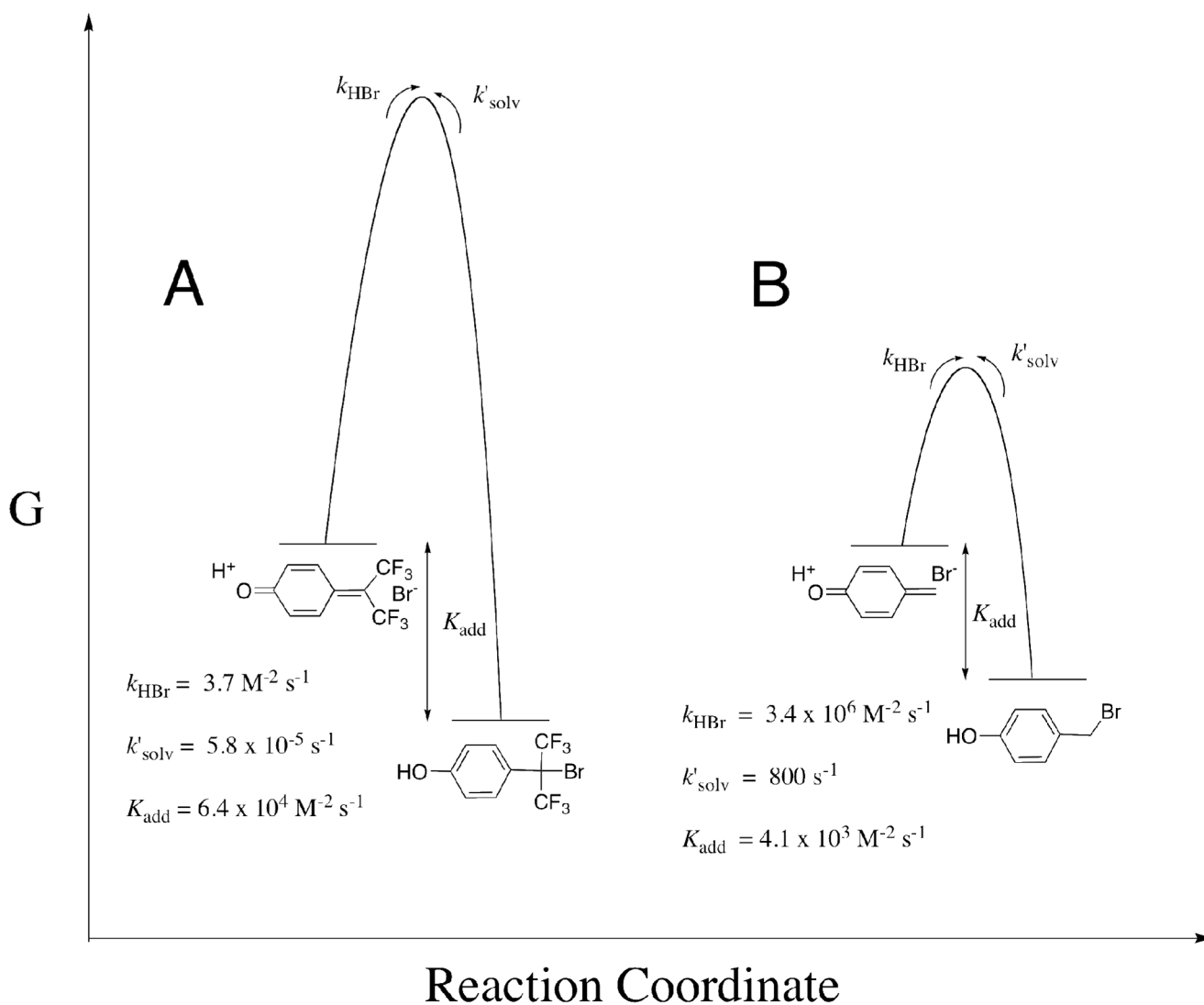


Figure 4.

(A) Free energy reaction profile for the reversible addition of Br^- to the di- α - CF_3 substituted quinone methide **48**, constructed using rate and equilibrium data from ref. 91. (B) Free energy reaction profile for the reversible addition of Br^- to the simple quinone methide **p-1**, constructed using rate and equilibrium data from ref. 52. These nucleophile addition reactions show similar thermodynamic driving force, but both the formation and reaction of **48** are slow because of the large intrinsic barrier Δ for nucleophile addition.

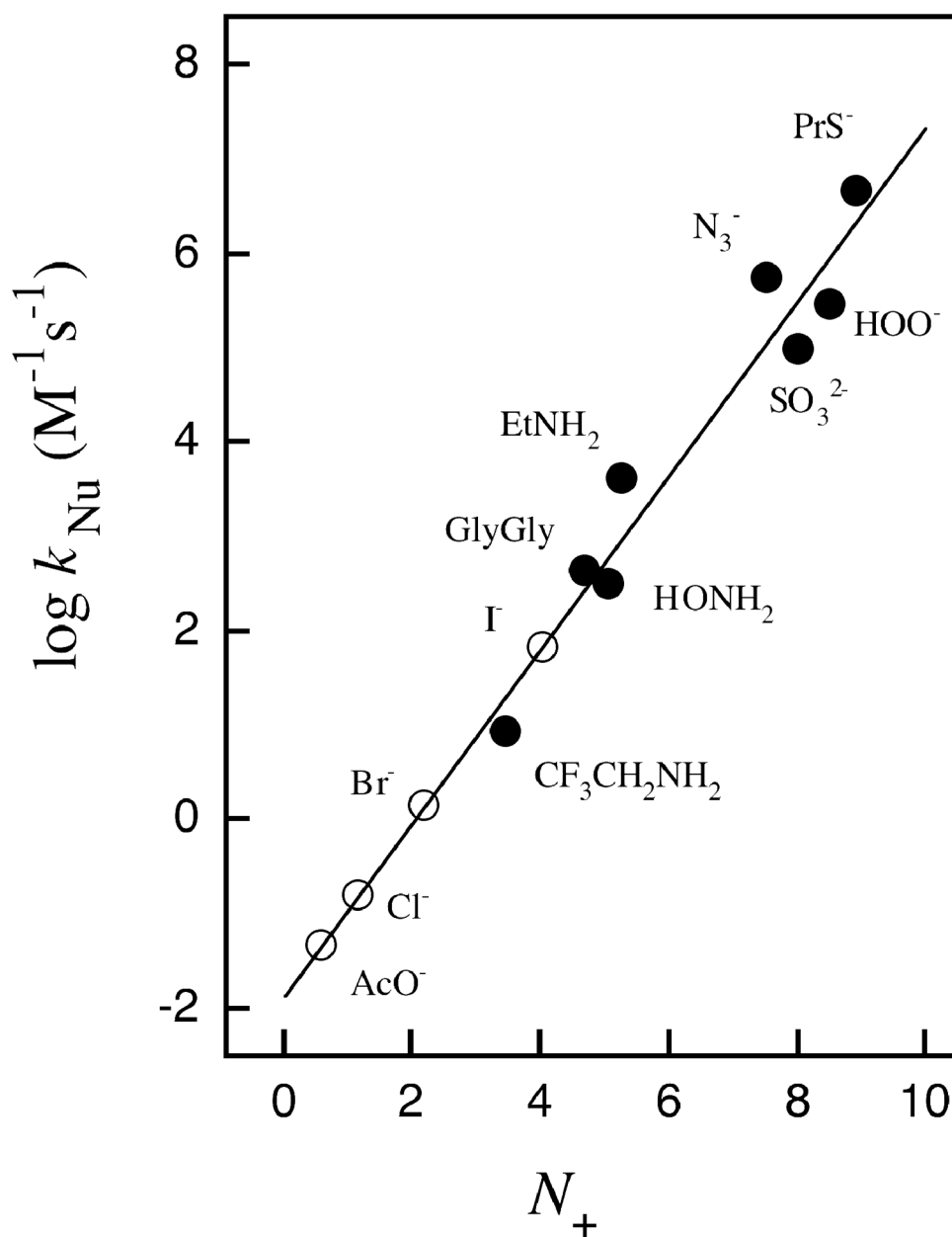
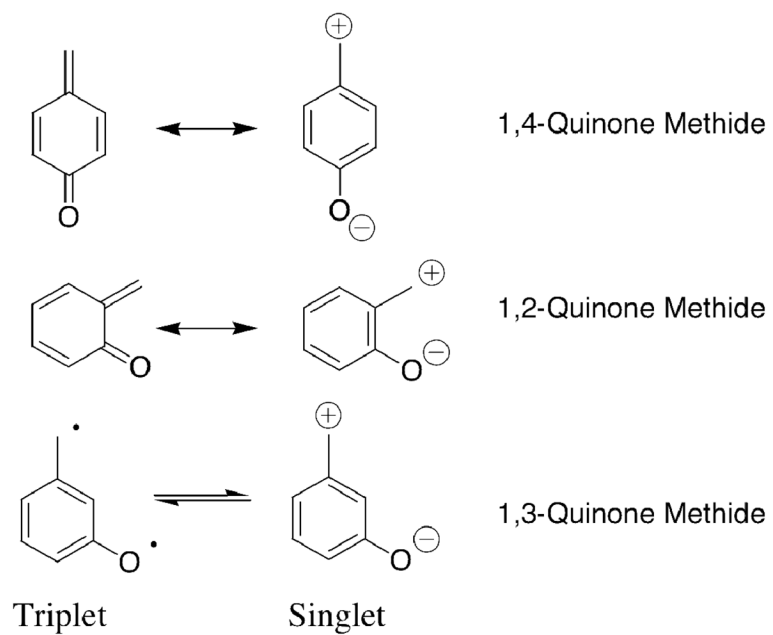
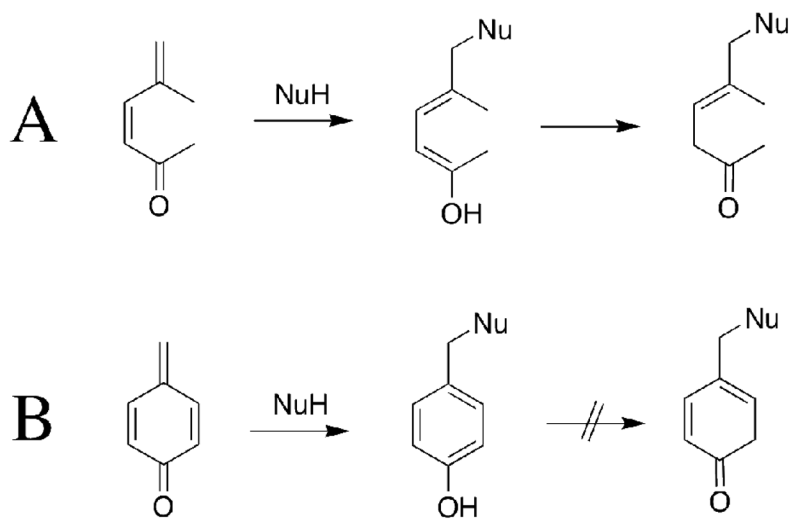


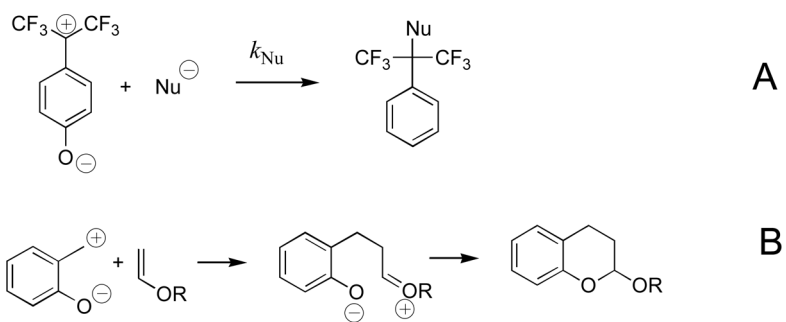
Figure 5. (A) Correlation of the second-order rate constants k_{Nu} ($M^{-1} s^{-1}$) for the addition of nucleophiles to **48** in water at 25 °C with Ritchie N_+ values.⁹¹ The solid symbols are the experimental data that were used to obtain the correlation line of slope 0.92 (0.10); the open symbols are the data for nucleophiles for which values of N_+ have not previously been determined and which are assumed to follow this correlation. [Reprinted with permission of the American Chemical Society from Ref. 4].

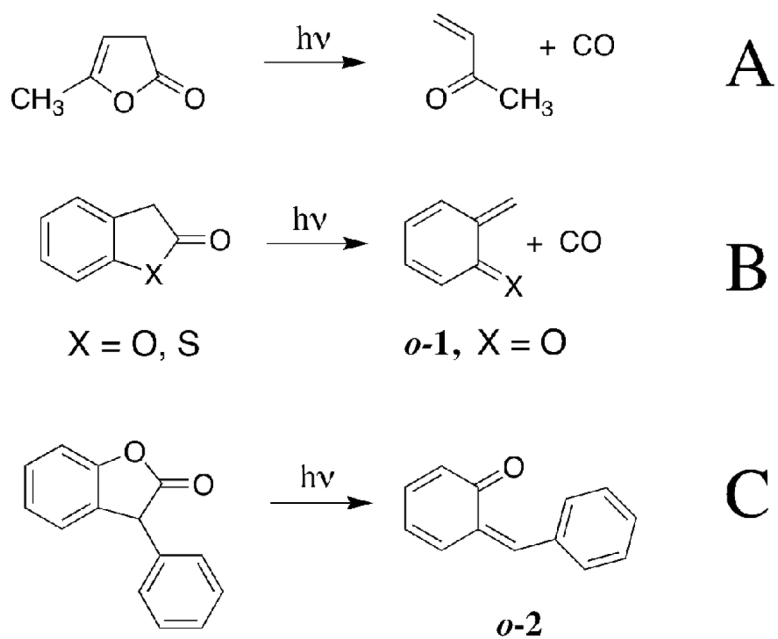


Scheme 1.

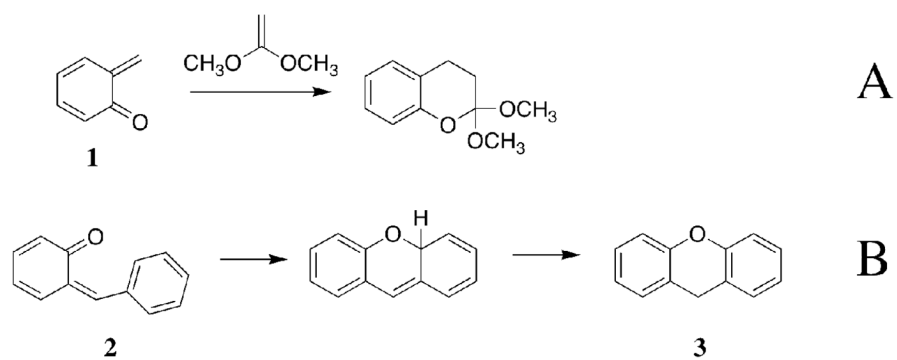


Scheme 2.

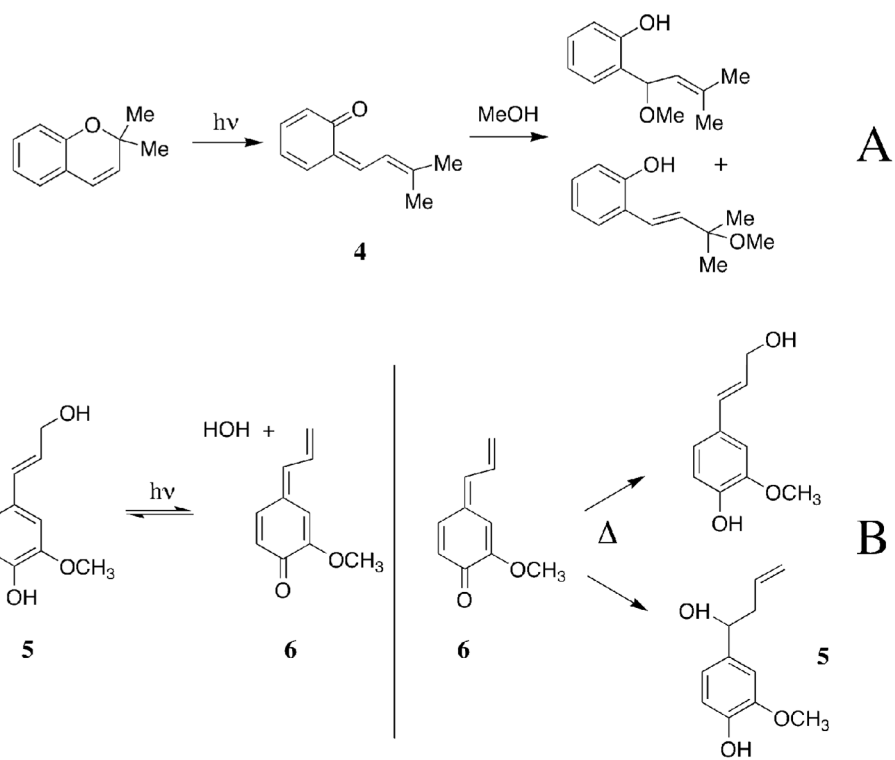
**Scheme 3.**



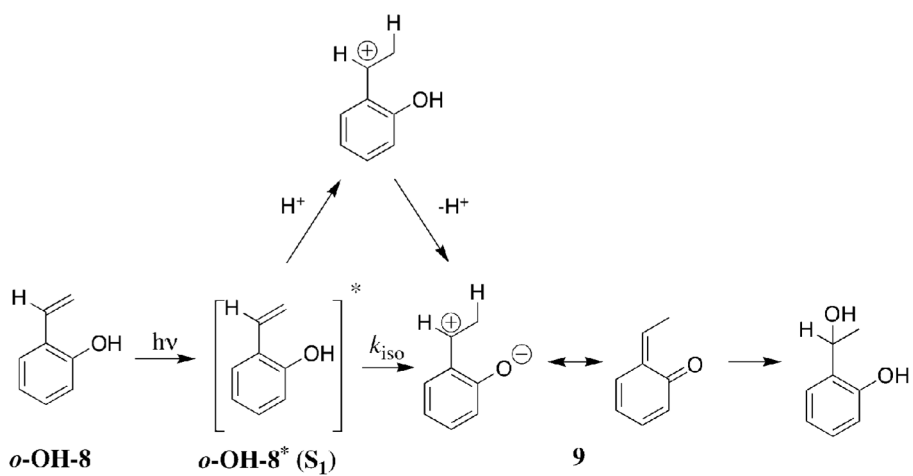
Scheme 4.



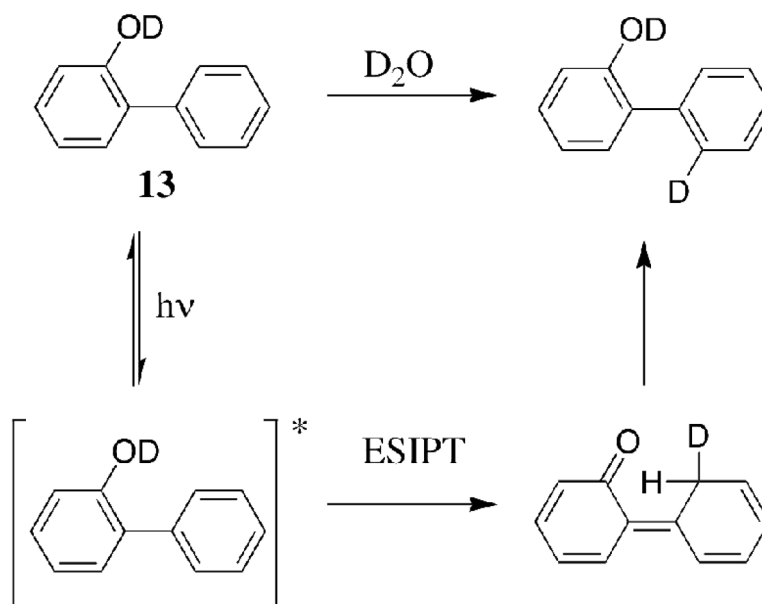
Scheme 5.



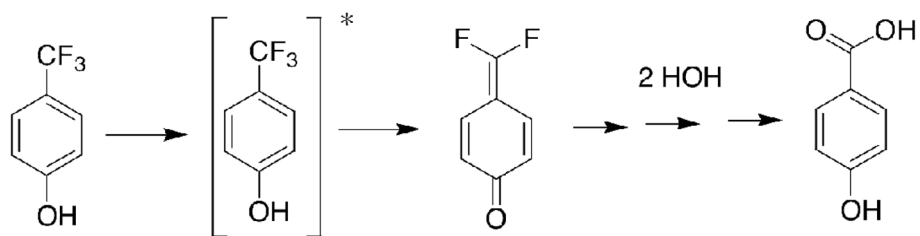
Scheme 6.



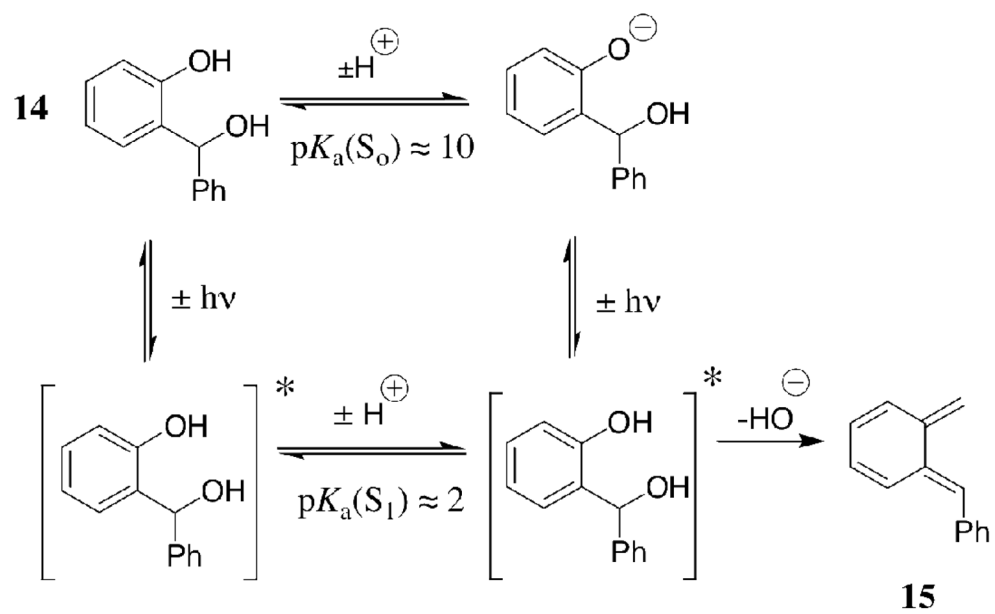
Scheme 7.



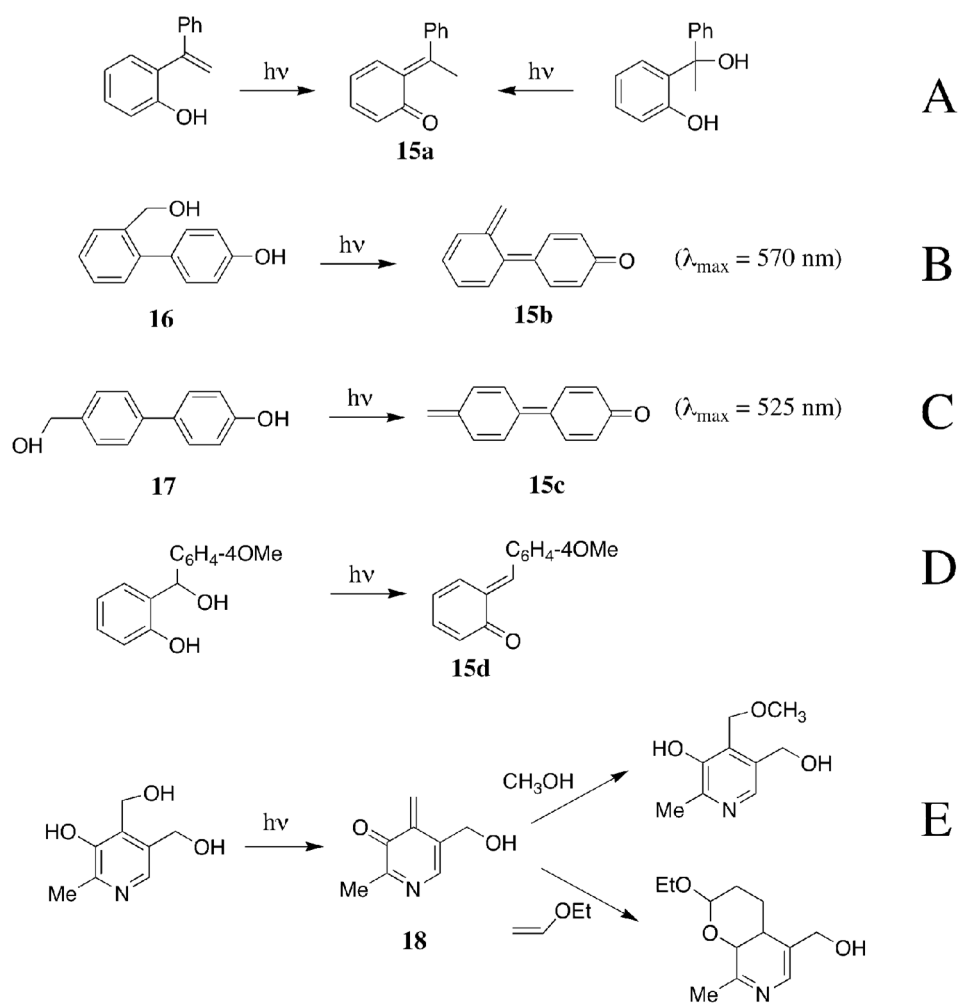
Scheme 8.



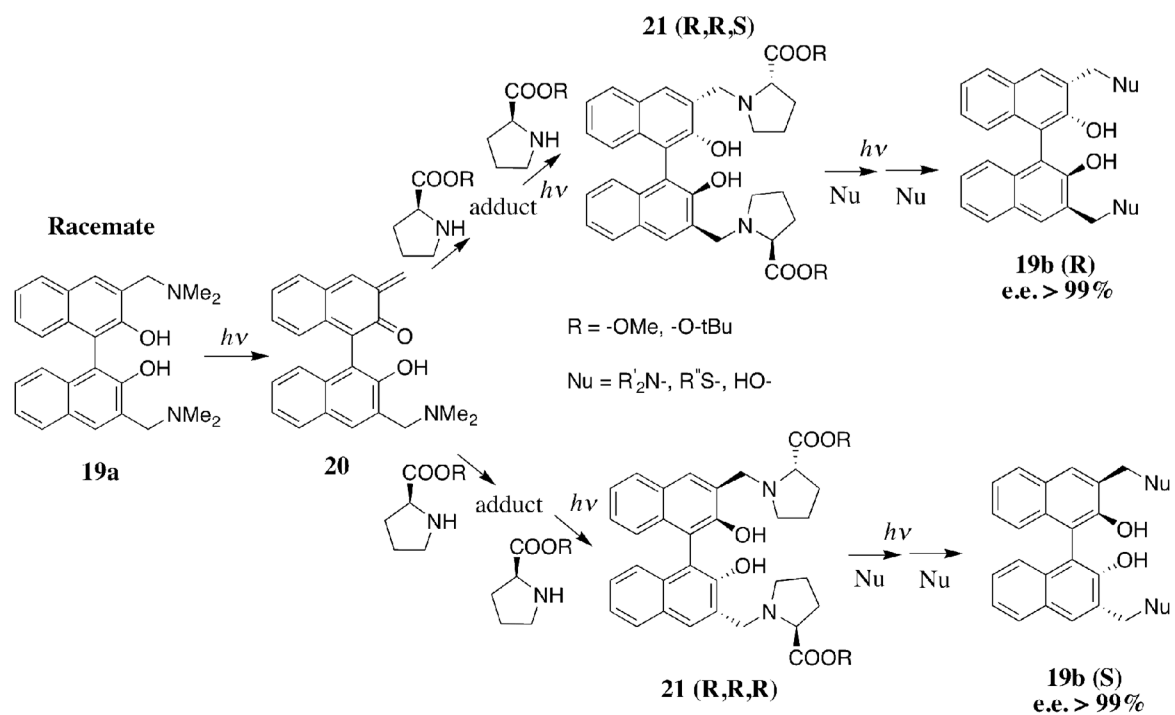
Scheme 9.



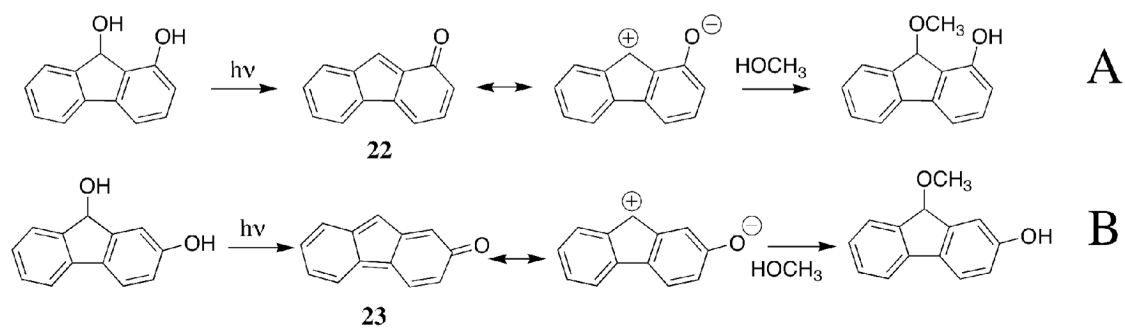
Scheme 10.



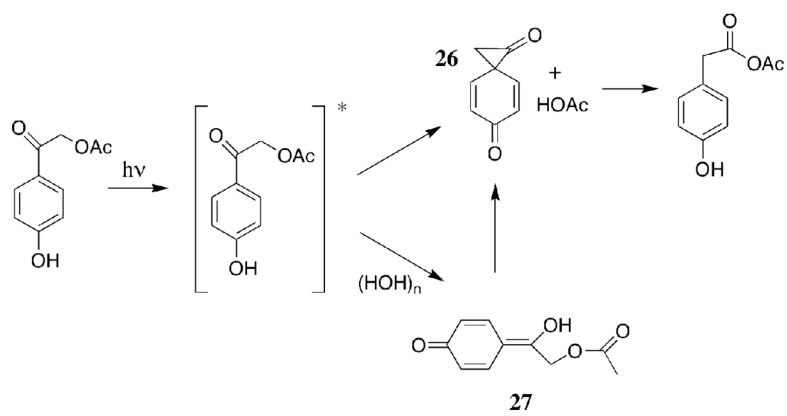
Scheme 11.



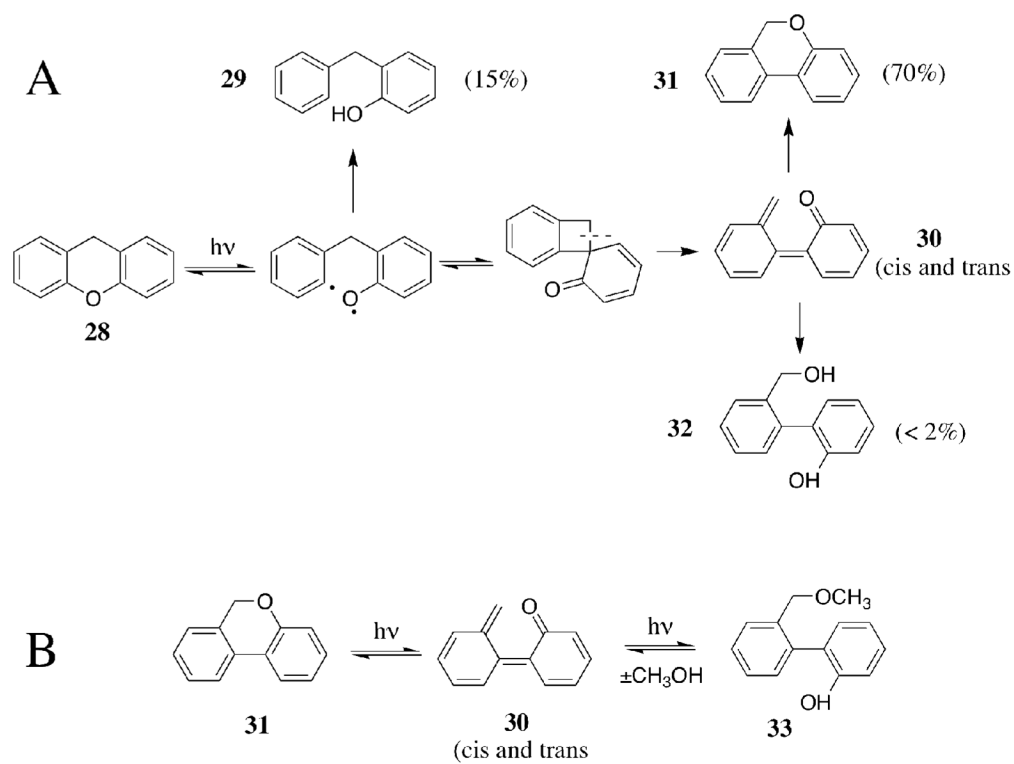
Scheme 12.



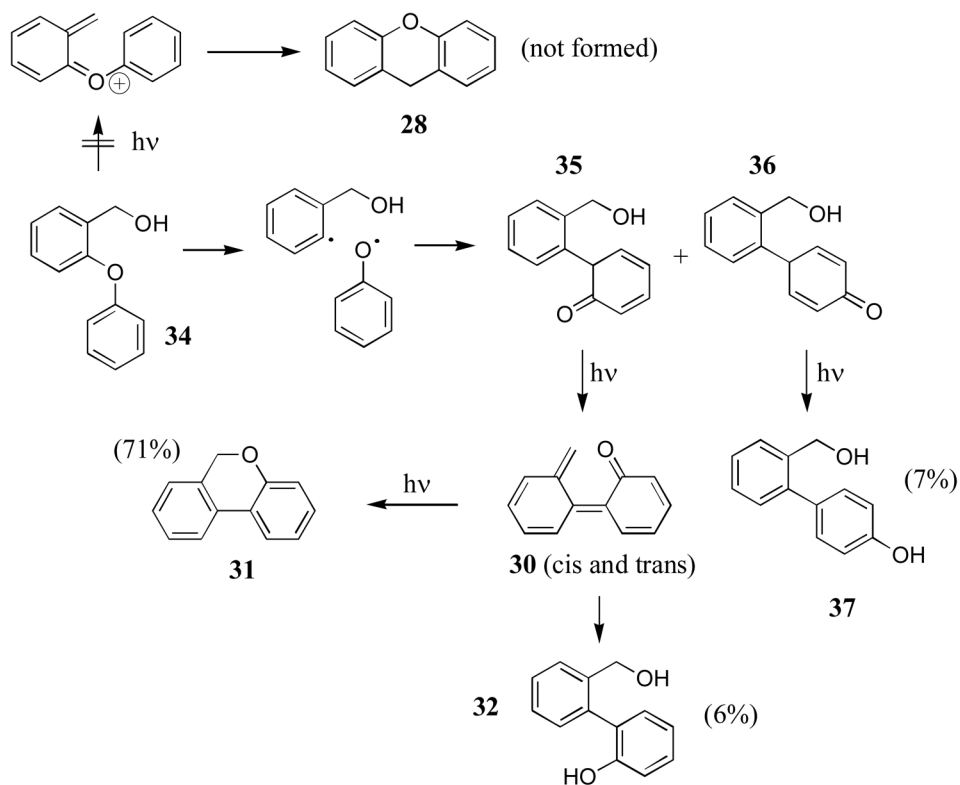
Scheme 13.



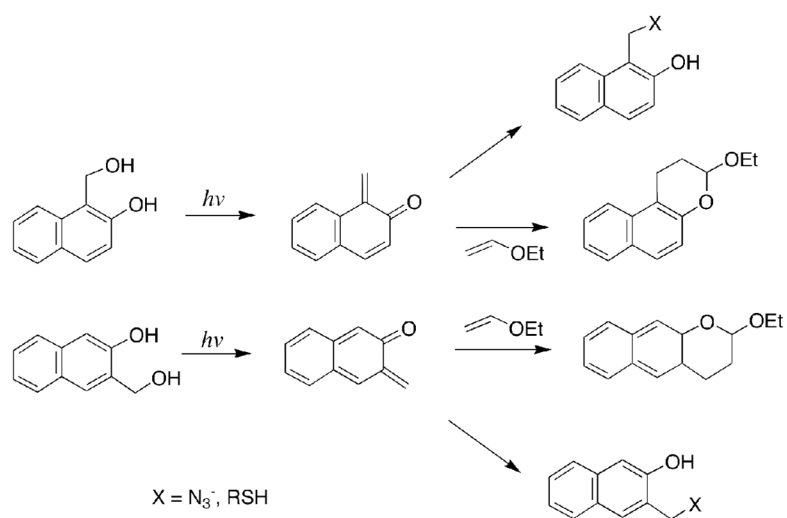
Scheme 15.



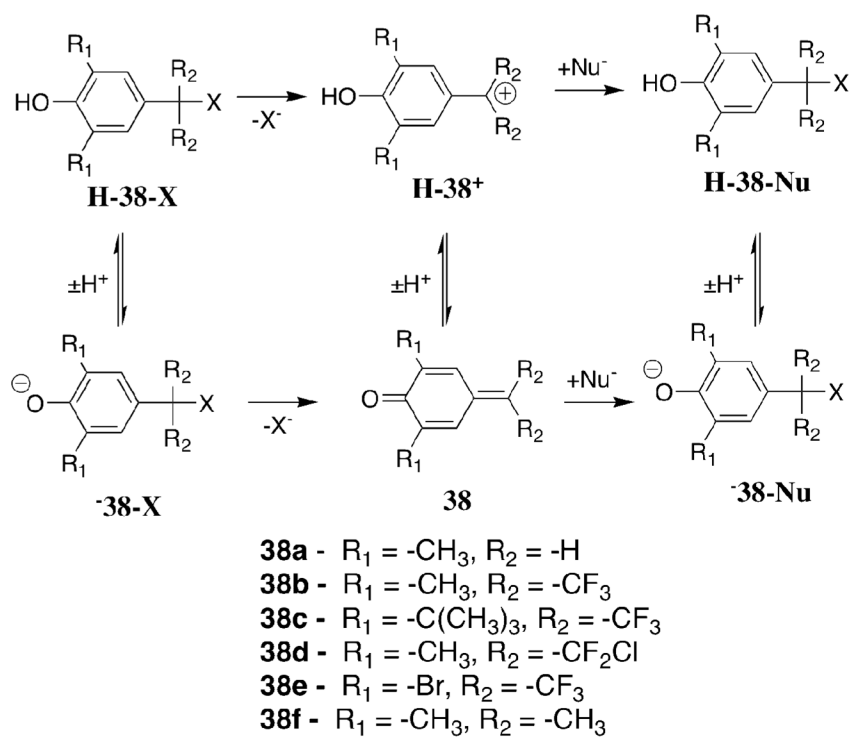
Scheme 16.



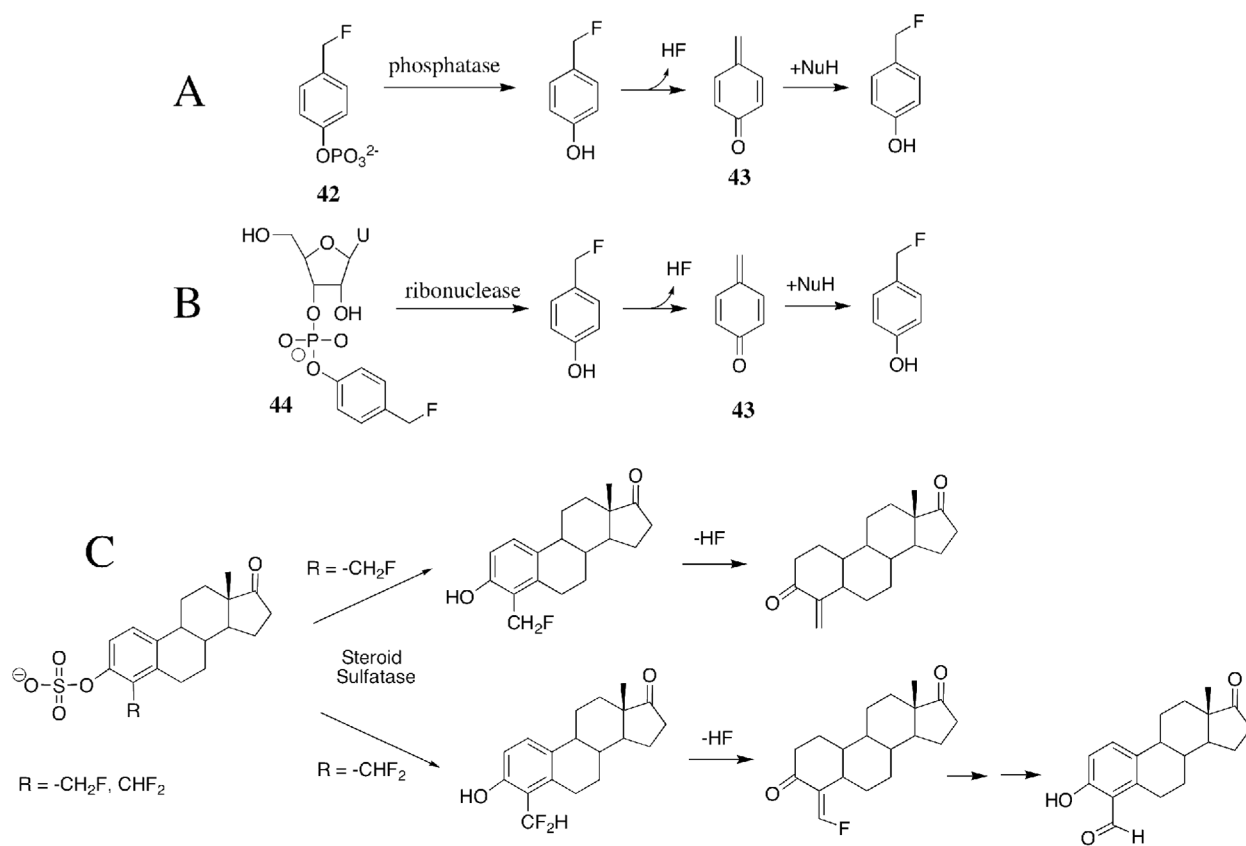
Scheme 17.



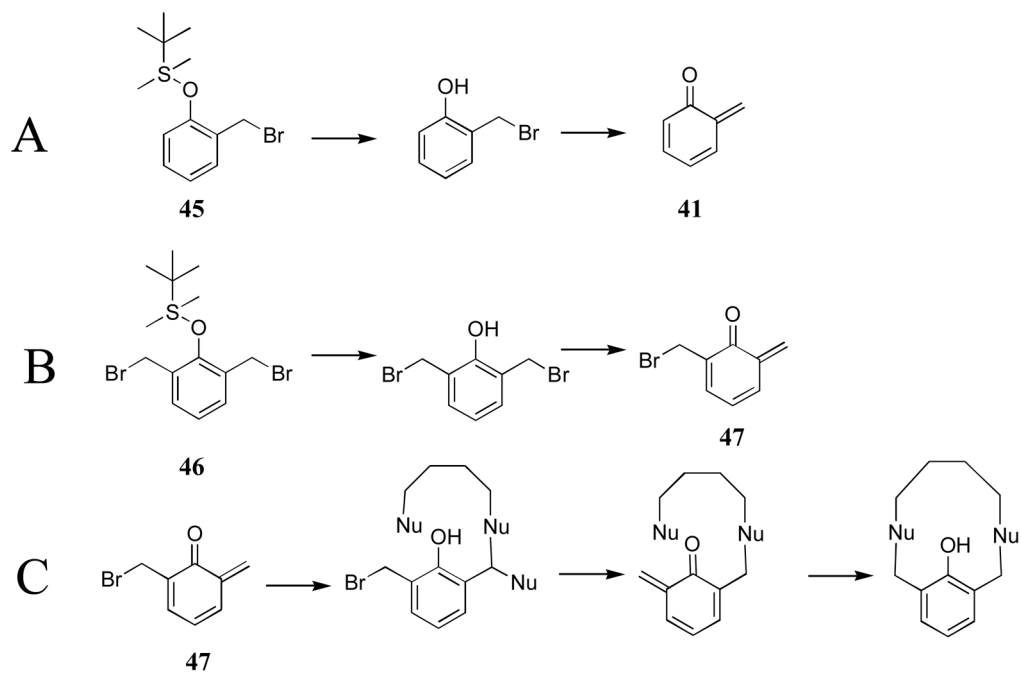
Scheme 18.



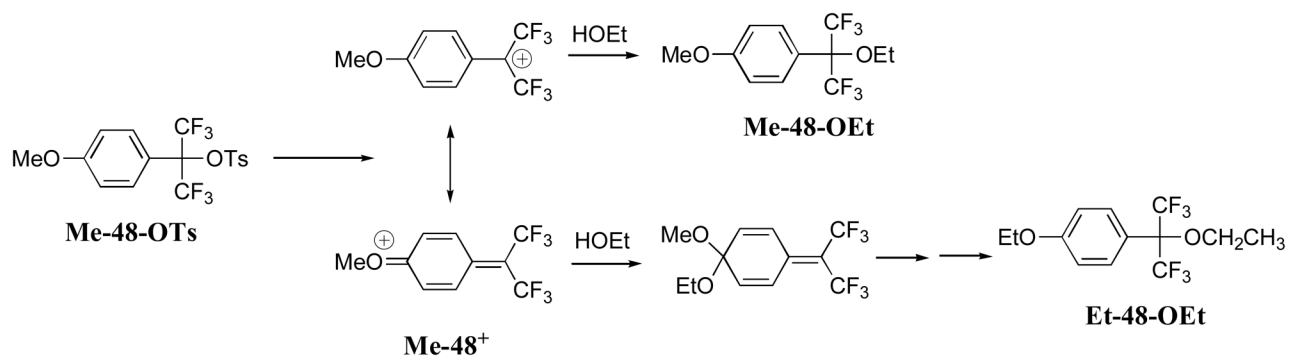
Scheme 19.



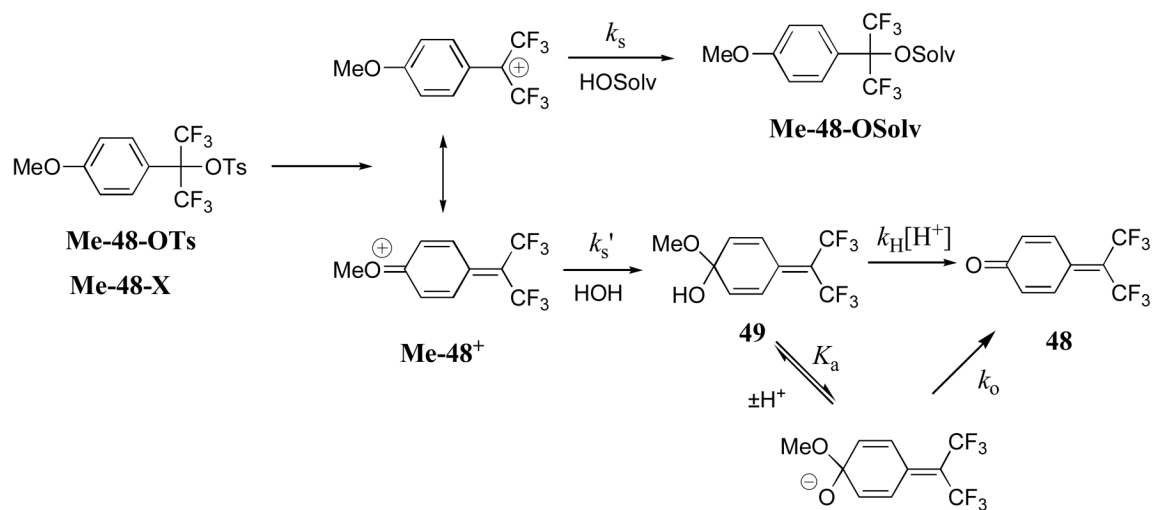
Scheme 20.



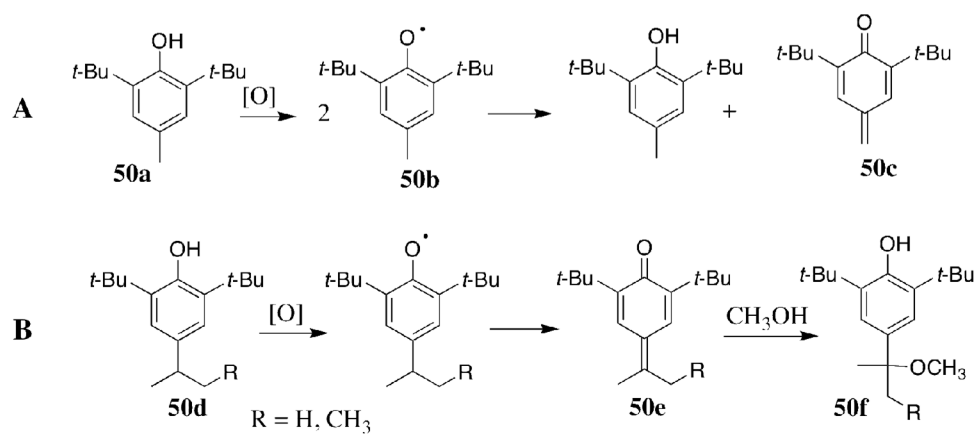
Scheme 21.



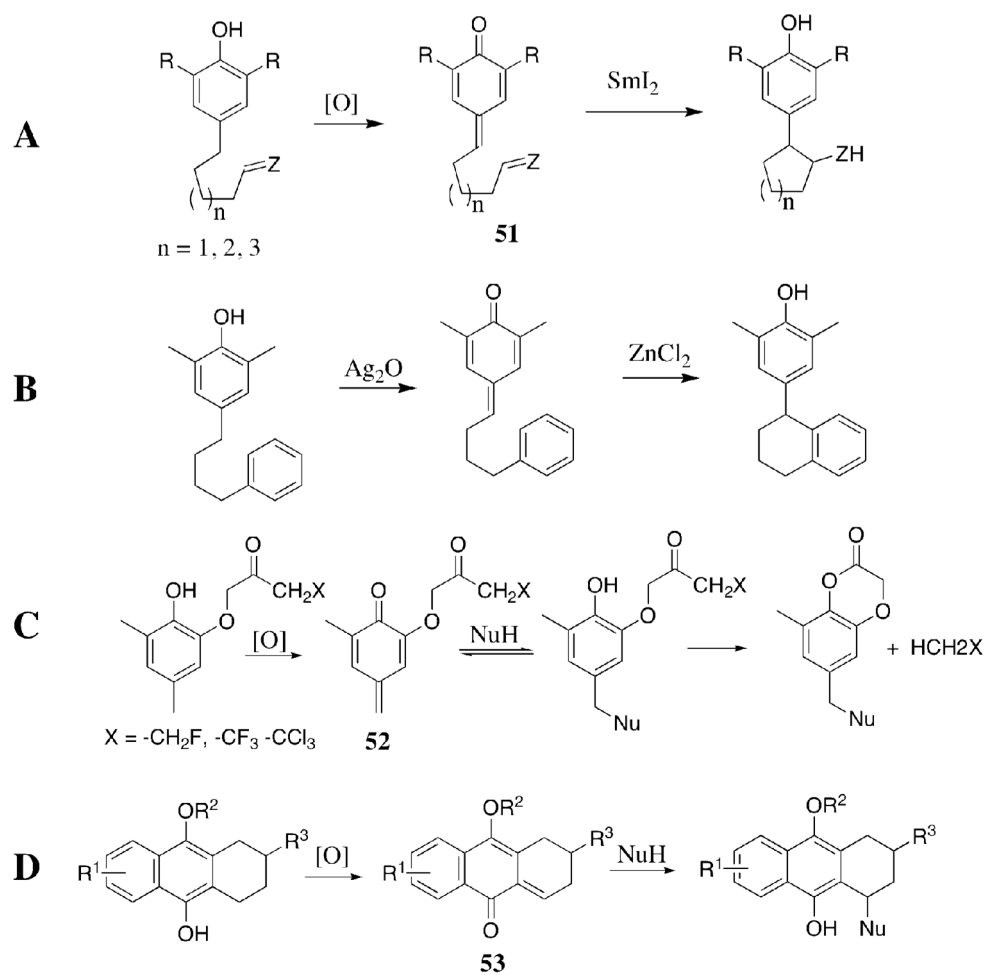
Scheme 22.



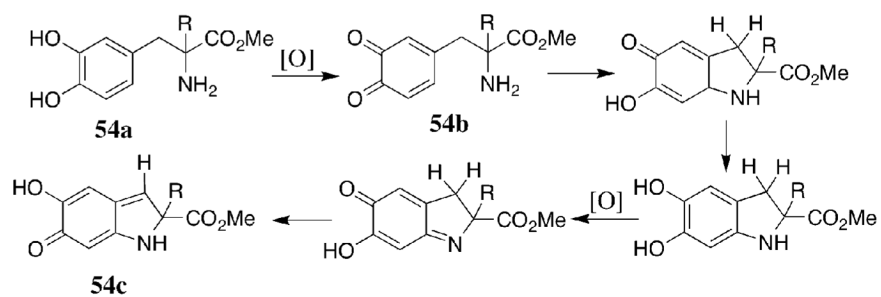
Scheme 23.



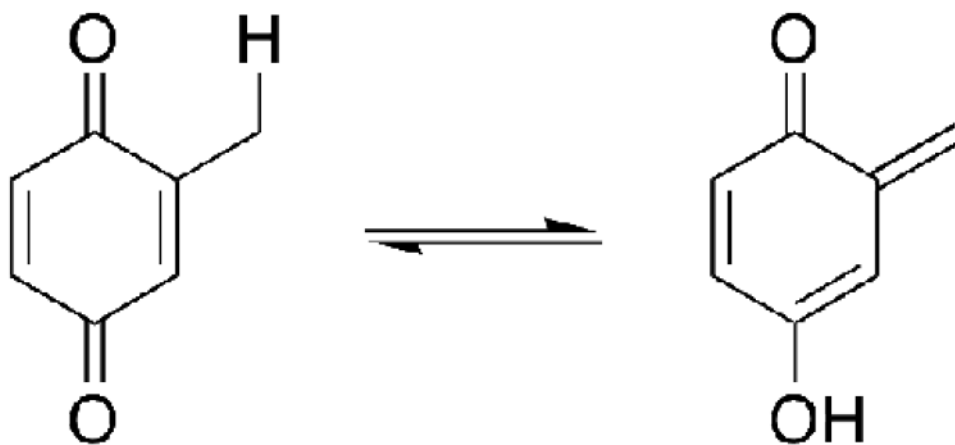
Scheme 24.



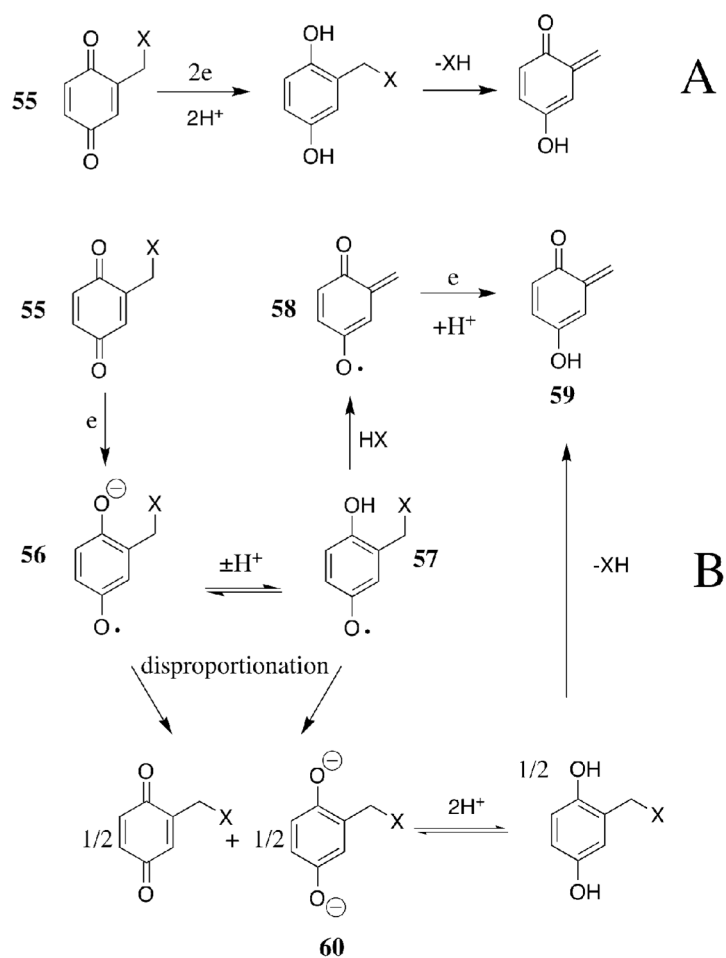
Scheme 25.



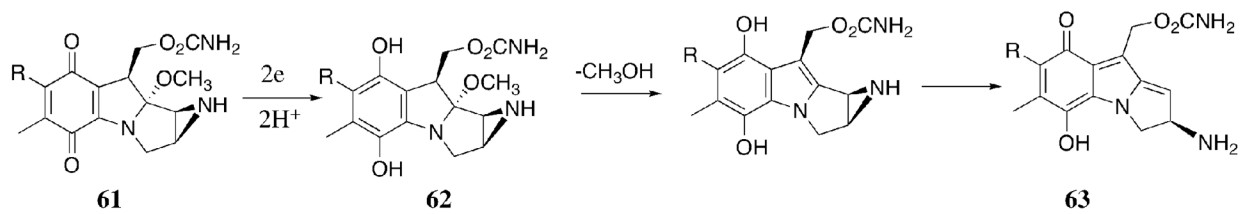
Scheme 26.



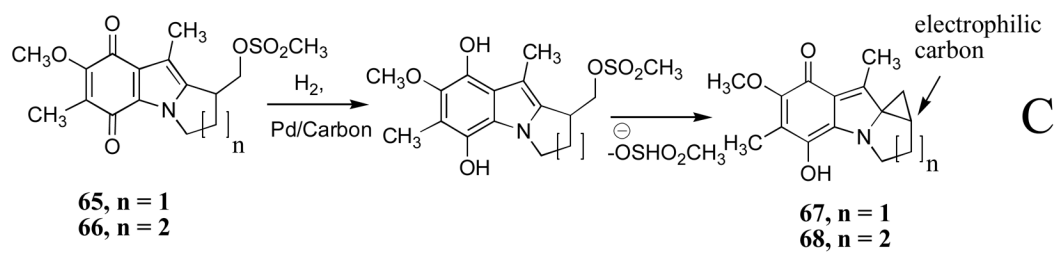
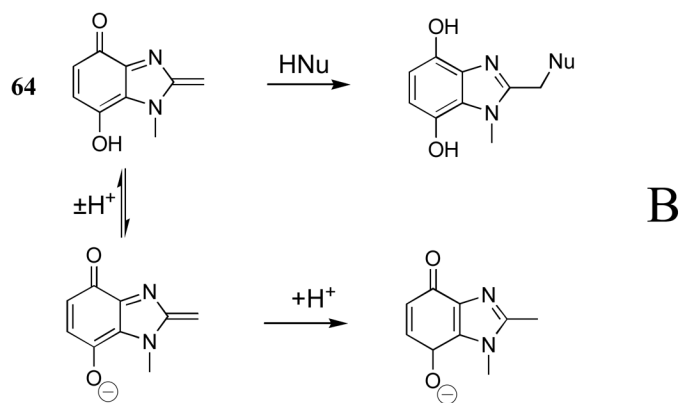
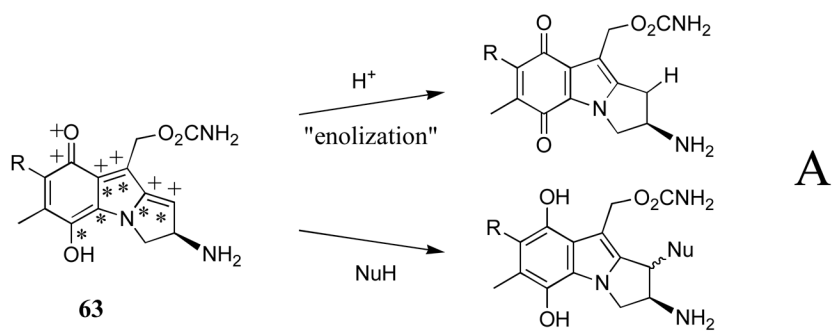
Scheme 27.



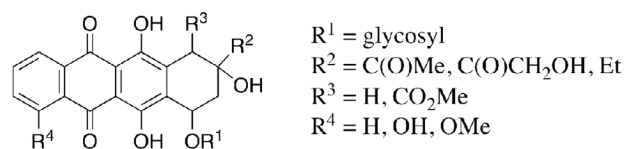
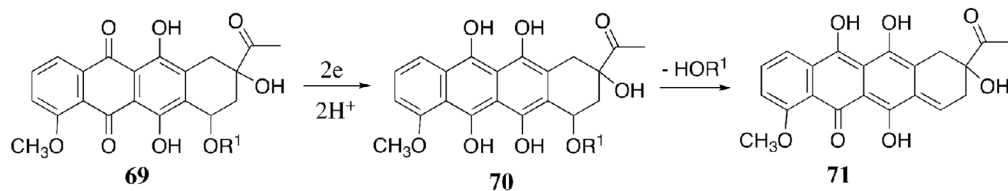
Scheme 28.

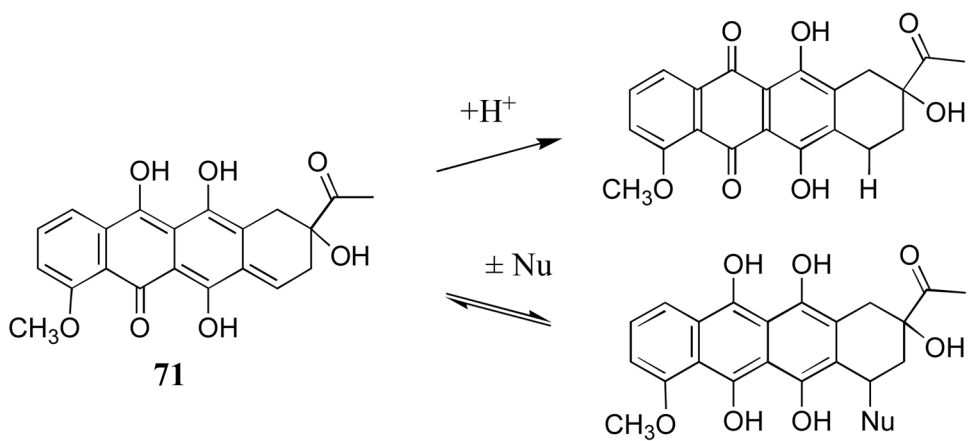
Mitomycin A: X = -OCH₃Mitomycin C: X = -NH₂

Scheme 29.

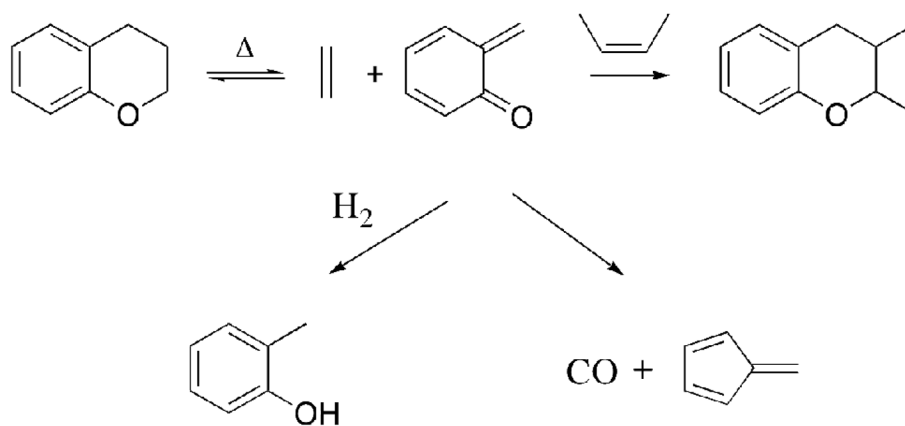


Scheme 30.

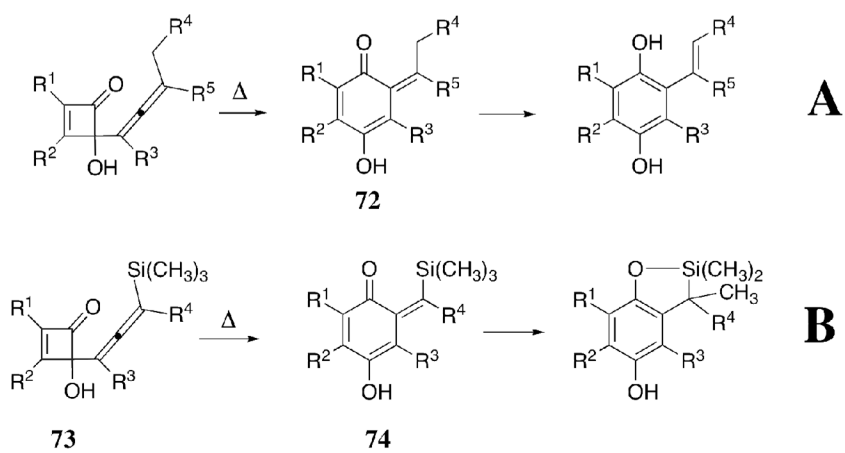
**69****69****70****71****Scheme 31.**



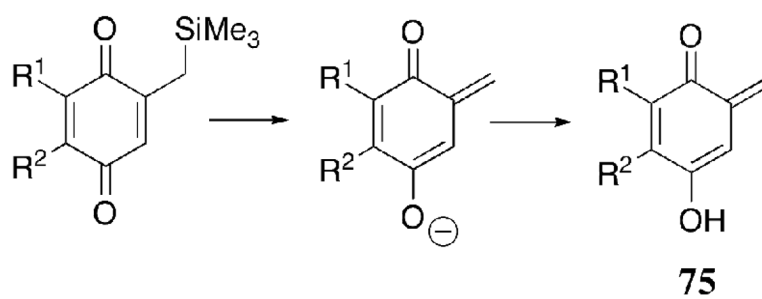
Scheme 32.



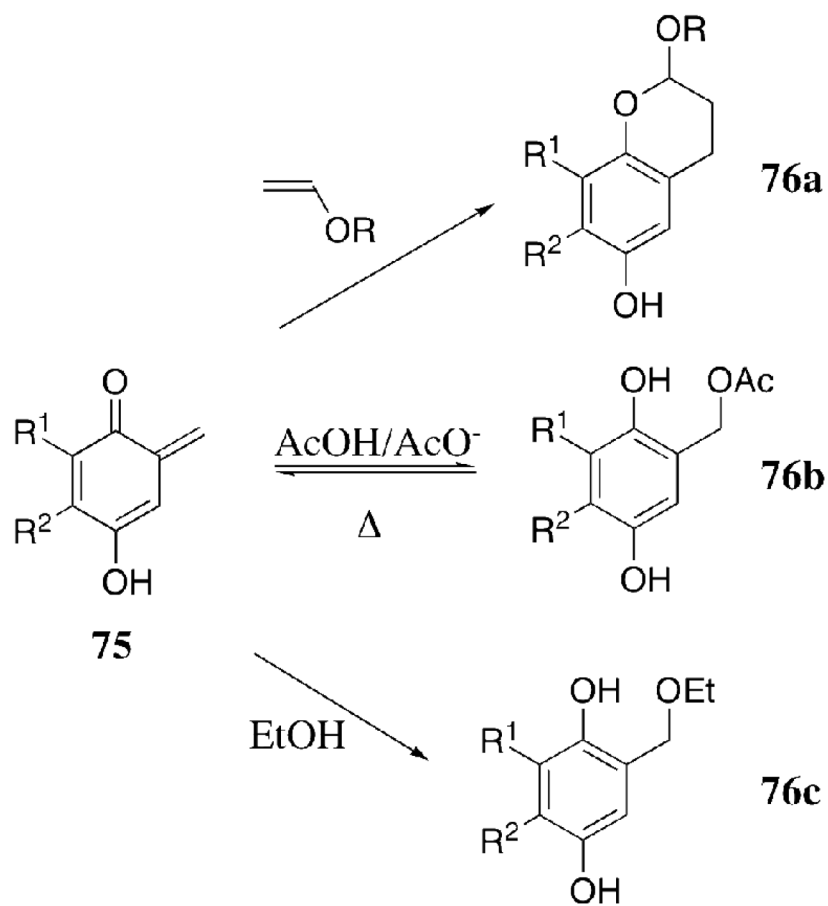
Scheme 33.



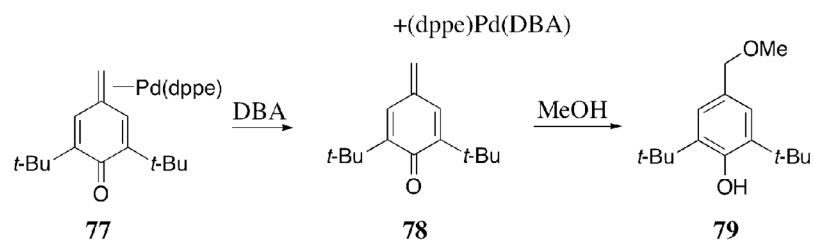
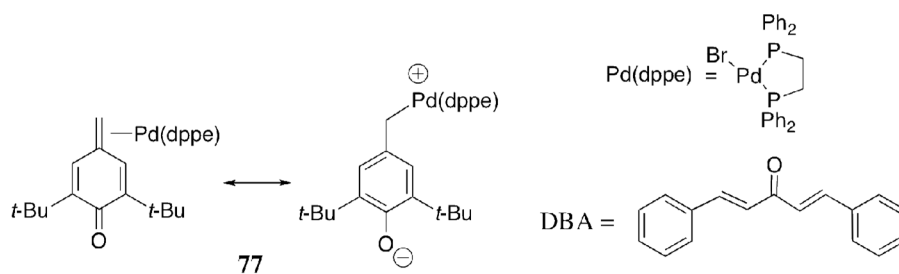
Scheme 34.



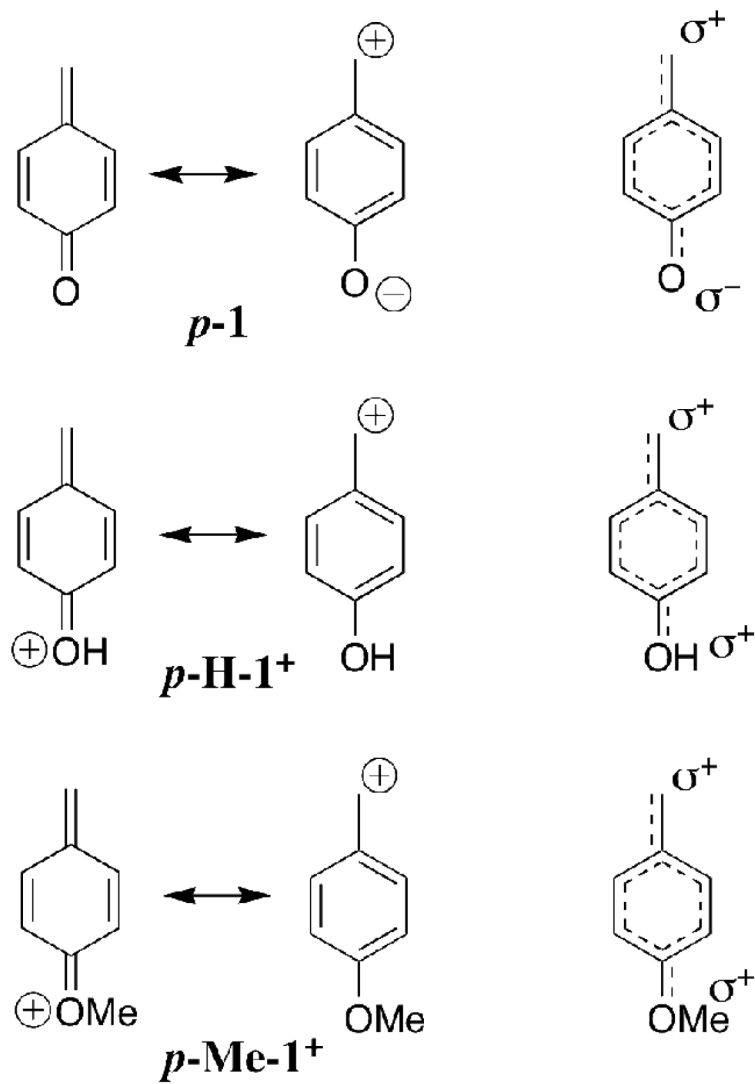
Scheme 35.



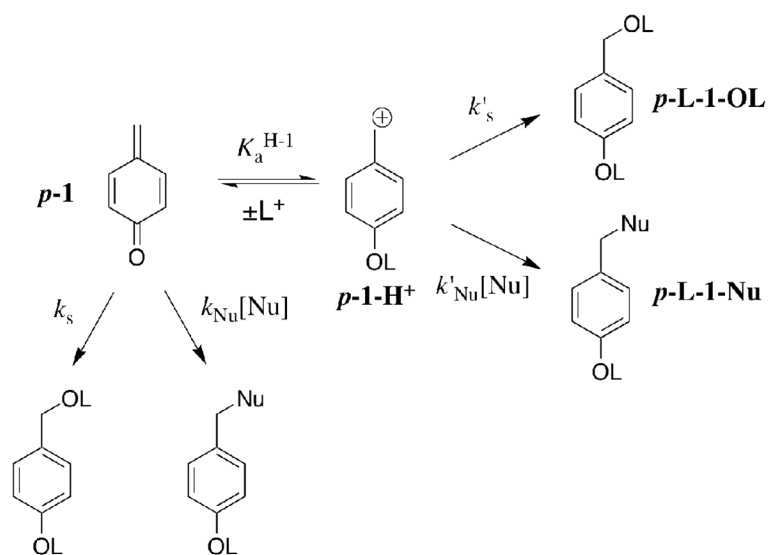
Scheme 36.



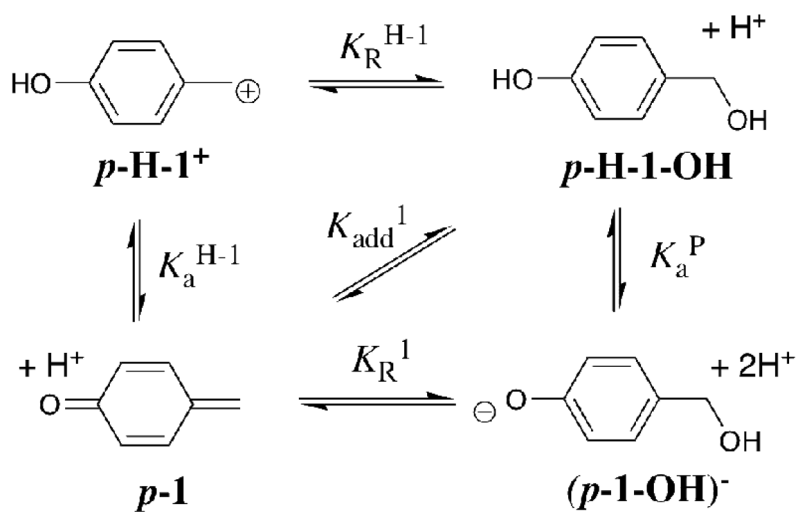
Scheme 37.



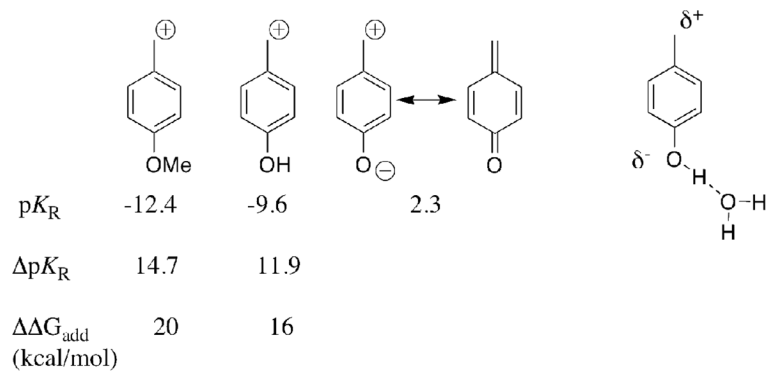
Scheme 38.



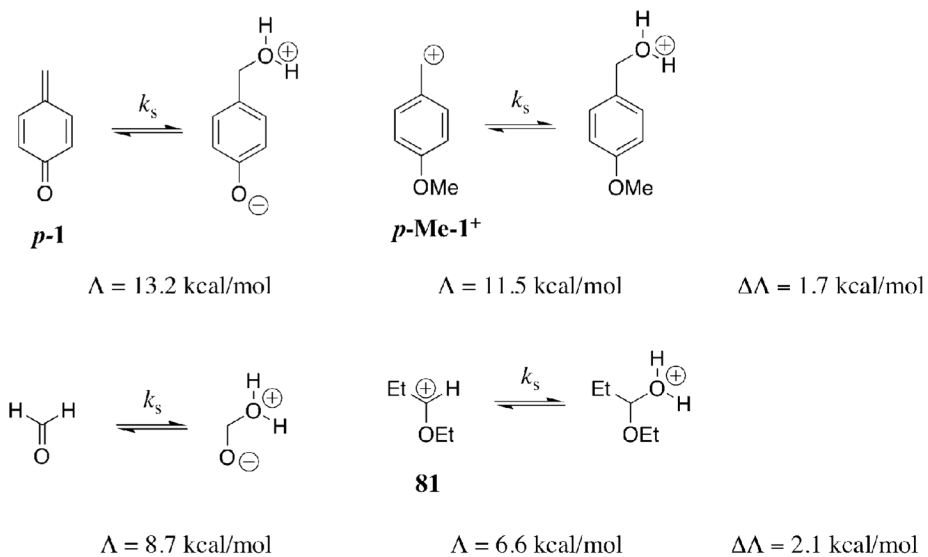
Scheme 39.



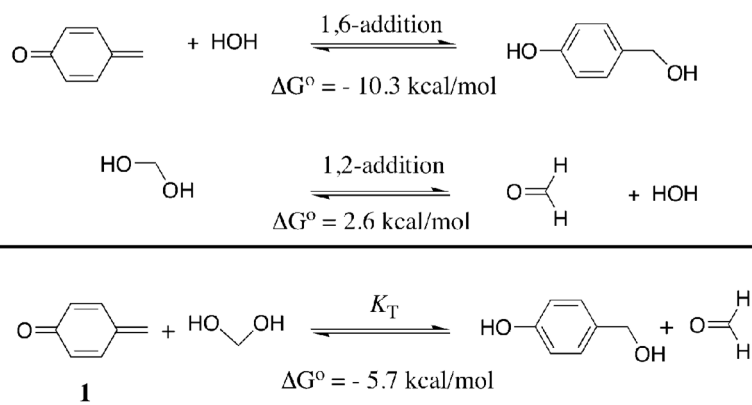
Scheme 40.



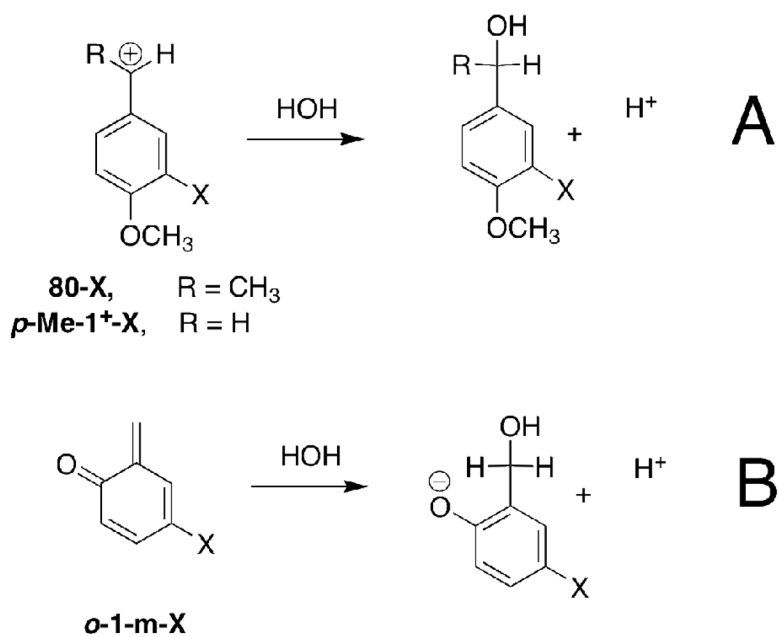
Scheme 41.



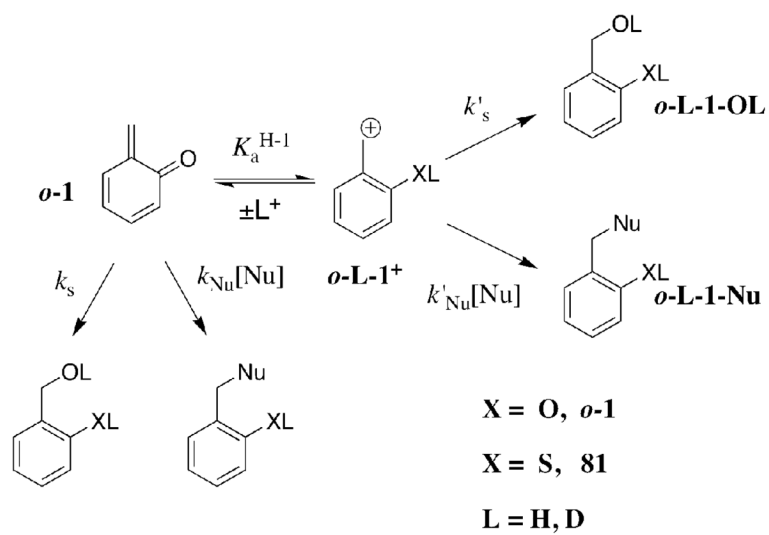
Scheme 42.



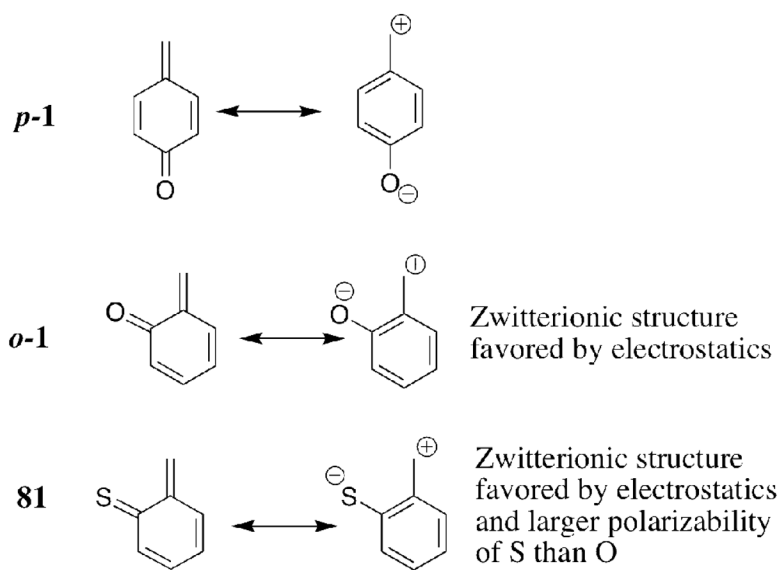
Scheme 43.



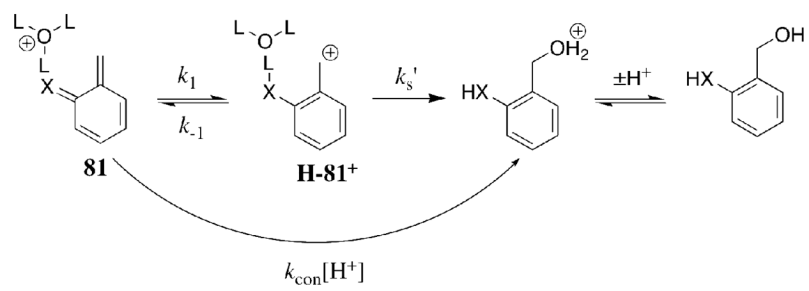
Scheme 44.



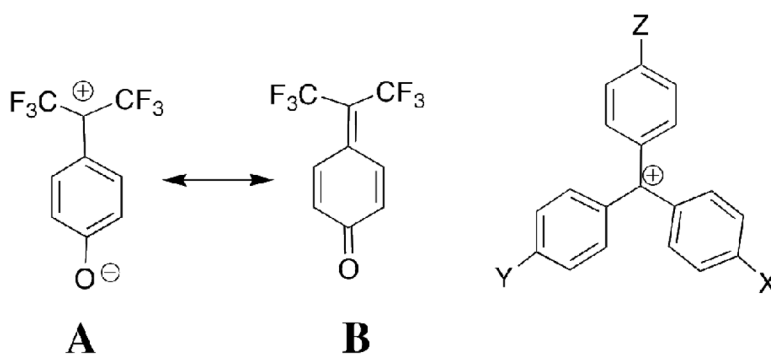
Scheme 45.



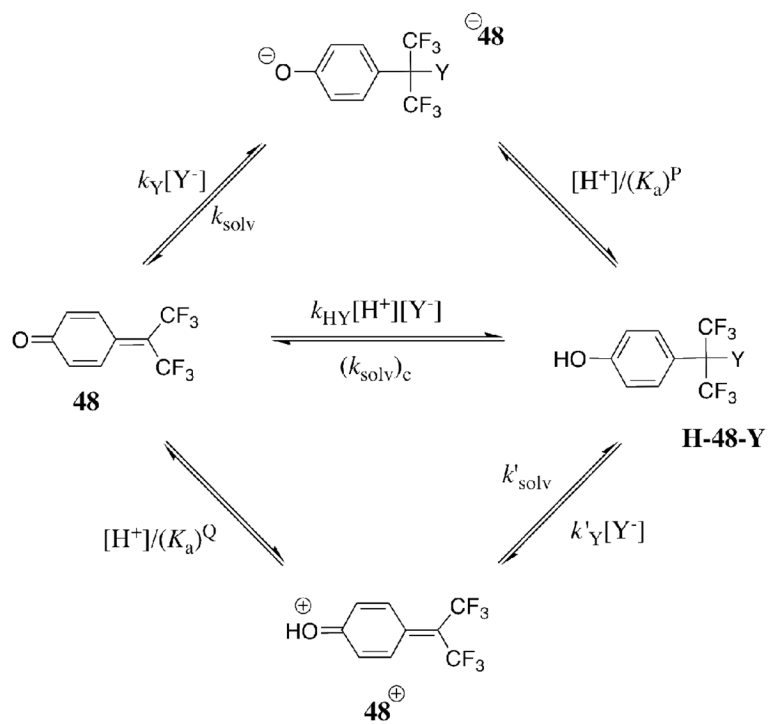
Scheme 46.



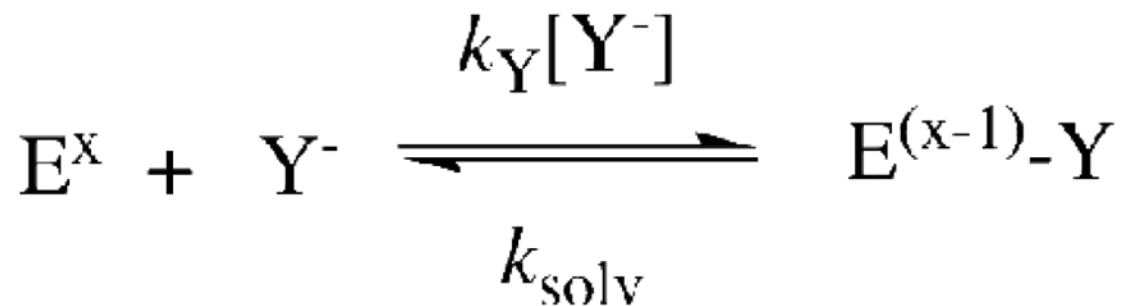
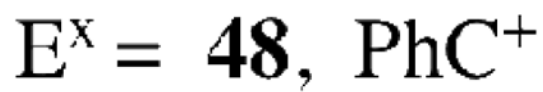
Scheme 47.



Scheme 48.

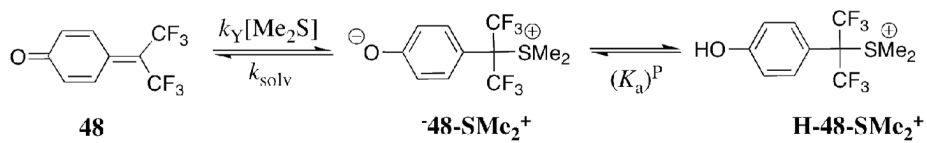


Scheme 49.



$$K_{\text{add}} = k_Y[Y^-]/k_{\text{solv}}$$

Scheme 50.



Scheme 51.

Table 1

Rate and equilibrium constants determined for the reactions of quinone methides with water in acidic solutions.

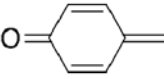
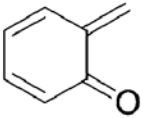
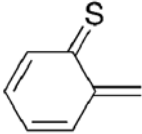
Quinone Methide	pK_a	k_s (s^{-1})	k_s' (s^{-1})	k_H ($M^{-1} s^{-1}$)
 <i>p</i> -1 (Ref 52)	-2.0	3.3	5.8×10^6	5.3×10^4
 <i>o</i> -1 (Ref 51)	-1.7	230	4×10^7	8.4×10^5
 81 (Ref 58)	< -3	1.2×10^5	not determined	7.0×10^4

Table 2

Equilibrium constants for Scheme 40, determined as described in the text, for addition of water to *p*-1 and to *p*-1-**H**⁺.³

Equilibrium	Constant	ΔpK
pK_R^1	2.3	11.9
pK_R^{H-1}	-9.6	
pK_a^P	9.9	11.9
pK_a^{H-1}	-2.0	
pK_{add}^1	7.6	

Table 3

Rate and Equilibrium Constants and Intrinsic Reaction Barriers [ref 91] for the Addition of Nucleophiles to the Quinone Methide **48** and the Triaryl[methyl] Carbocation (PhC^+) in Water at 25° C. The rate and equilibrium constants are defined in Scheme 50.⁹¹

Electrophile	k_{Nu} ($\text{M}^{-1} \text{s}^{-1}$)	K_{add} (M^{-1})	k_{solv} (s^{-1})	ΔG^\ddagger (kcal/mol)	$\Delta\Delta G^\ddagger$ (kcal/mol)	Δ (kcal/mol)	$\Delta\Delta$ (kcal/mol)
Cl- + 48	0.16	$\approx 4 \times 10^{-5}$	$\approx 4 \times 10^3$	6.0	8.5	15.4	5.4
Cl- + PhC^+	2.2×10^6	70	3×10^4	-2.5		10	
Br- + 48	1.4	2.4×10^{-5}	6×10^4	6.3	7.4	13.9	5.0
Br- + PhC^+	5×10^6	6	8×10^5	-1.1		8.9	
I- + 48	68	2.4×10^{-4}	3×10^5	4.9		12.4	
AcO- + 48	0.048	≈ 8	≈ 0.006	-1.2	9.4	19.8	5.2
AcO- + PhC^+	4×10^5	6×10^7	7×10^{-3}	-10.6		14.6	